Gallium(III)-pyridoxal thiosemicarbazone derivatives as nontoxic agents against Gram-negative bacteria

OXFORD UNIVERSITY PRESS | Metallomics

Gallium(III)-Pyridoxal Thiosemicarbazone Derivatives as Nontoxic Agents against Gram Negative Bacteria

Journal:	*Metallomics Journal*
Manuscript ID	Draft
Manuscript Type:	Paper
Date Submitted by the Author:	n/a
Complete List of Authors:	Scaccaglia, Mirco; University of Parma, Department of Chemistry, Life Sciences and Environmental Sustainability Rega, Martina; University of Parma, Department of Veterinary Science Vescovi, Marianna; University of Parma, Department of Chemistry, Life Sciences and Environmental Sustainability Pinelli, Silvana; University of Parma, Department of Medicine and Surgery Tegoni, Matteo; University of Parma, Department of Chemistry, Life Sciences and Environmental Sustainability Bacci, Cristina; University of Parma, Department of Veterinary Science Pelosi, Giorgio; University of Parma, Department of Chemistry, Life Sciences and Environmental Sustainability; University of Parma, CERT, Center of Excellence for Toxicological Research Bisceglie, Franco; University of Parma, Department of Chemistry, Life Sciences and Environmental Sustainability; University of Parma, CERT, Center of Excellence for Toxicological Research
Keywords:	Antimicrobial resistance, gallium(III), thiosemicarbazone, solution equilibria, Gram negative, pyridoxal

Gallium(III)-Pyridoxal Thiosemicarbazone Derivatives as Nontoxic Agents against Gram Negative Bacteria

Mirco Scaccaglia[1], Martina Rega[2], Marianna Vescovi[1], Silvana Pinelli[3], Matteo Tegoni[1], Cristina Bacci[2], Giorgio Pelosi[1,4] and Franco Bisceglie[1,4]*

[1] Department of Chemistry, Life Sciences and Environmental Sustainability, University of Parma, 43124 Parma, Italy;

[2] Department of Veterinary Science, University of Parma, Strada del Taglio 10, 43126 Parma, Italy;

[3] Department of Medicine and Surgery, University of Parma, Via Gramsci 14, 43126 Parma, Italy;

[4] CERT, Center of Excellence for Toxicological Research, University of Parma, 43124 Parma, Italy

* corresponding author: franco.bisceglie@unipr.it

Abstract

Many bacterial strains are developing mechanism of resistance to antibiotics, rendering last-resort antibiotics inactive. Therefore, new drugs are needed and in particular metal-based compounds represent a valid starting point to explore new antibiotic classes. In this study we have chosen to investigate gallium(III) complexes for their potential antimicrobial activity against different strains of *Klebsiella pneumoniae*, *Escherichia coli* and *Pseudomonas aeruginosa* which have developed different type of resistance mechanism, including the expression of β-lactamases (NDM-1, ESβL or AmpC) or the production of biofilm. We studied a series of thiosemicarbabazones derived from pyridoxal, their related Ga(III) complexes, and the speciation in solution of the Ga(III)/ligand systems as a function of the pH. Proton dissociation constants and conditional stability constants of Ga(III) complexes were evaluated by UV/Vis spectroscopy, and the most relevant species at physiological pH were identified. Cytotoxicity experiments showed that the compounds are active against resistant Gram-negative strain with minimal inhibitory concentration in the μM range, while no cytotoxicity was detected in eukaryotic cells.

Keywords

Antimicrobial resistance, gallium(III), thiosemicarbazone, solution equilibria, Gram negative, pyridoxal

Introduction

Drug-resistant bacteria remain a major risk to human and animal's health. Misuse of antibiotics is the main cause of antimicrobial resistance (AMR), and this is also compromising lifesaving medical interventions. This global public health threat reflects in 670.000 resistant infections and at least 33.000 deaths in Europe each year.[1] Chromosomal genes mutations or exogenous resistances acquired by mobile genetic elements are the main sources of the spread of AMR, and bacteria can simultaneously acquire resistances to several antimicrobial agents. This is particularly risky as it may limit severely the available treatment alternatives for these infections.[2] From the evidence that AMR can spread between humans, animals and the environment, innovative approaches are necessary and new drugs are needed to be developed for the treatment of multidrug-resistant bacterial infections.[3,4]

The World Health Organization (WHO) create a list of Critically Important Antimicrobials (CIAs), molecule whose effectiveness for human medicine should not be compromised. Despite this Antimicrobial Resistance (AMR) related to those antibiotics have been found and their prevalence needs to be monitored.[5] In this study, resistance to 3rd, 4th generation cephalosporin and carbapenems, β-lactams antibiotics, were taken into account. Bacteria become resistant to β-lactams due to their ability to produce β-lactamases, enzymes that hydrolyse the β-lactam ring deactivating the molecule.[6] The most common β-lactamases are Extended-Spectrum β-lactamases (ESβL), AmpC β-lactamases and carbapenemases. Their biosynthesis is harboured by various genes mostly related to plasmid mobile elements. The dissemination of AMR can be also associated also with the ability to produce biofilm.[7] This microbial communities live in a self-made extracellular polymeric matrix and are able to maintain stable growth in stressful environmental condition. Moreover, these biofilm populations can acquire additional antibiotic resistances from other organisms by horizontal gene transfer facilitating AMR diffusion.[8]

Metal based compounds represent a valid scaffold to explore new antibiotic classes, because of their higher hit-rate when compared to simply organic molecules and of the emerging number of structure-activity relationship data.[9,10] Gallium(III) has chemical analogies with iron(III), and it can be incorporated in both eukaryotic and prokaryotic organisms as an iron(III) mimic, and can be targeted to iron-dependant proteins. Ga(III) does not have redox activity in physiological conditions and can interfere with iron metabolism, generating oxidative stress.[11] Gallium nitrate is FDA-approved as Ganite® formulation as a bone resorption inhibitor. Moreover, gallium(III) salts have been studied for their antimicrobial properties in several strains, and have shown a promising activity.[11–14]

In this context, we have decided to focus our investigation on gallium(III)-complexes. Thiosemicarbazone and semicarbazone derivatives were chosen as coordinating ligands because they represent a good scaffold for the design of bioactive complexes.[15–17] In our recent works, we already detected the antimicrobial activity of a series of quinolone- and cinnamaldehydethiosemicarbazone analogues against multi drugs resistant bacteria strains.[18,19] In this work, we have introduced, in the design of the ligands, the pyridoxal moiety, which is known for its crucial role in metabolic processes in prokaryotic and eukaryotic cells, and very recently used in resistant pathogens for the identification of new bacterial targets.[20] Pyridoxal is part of the group of vitamin B6, which also includes pyridoxine, pyridoxamine and their respective 5'-phosphates. In animal tissue the prevalent form of vitamin B6 is pyridoxal phosphate, which represents the active form. The absorption is regulated by phosphatase-mediated hydrolysis, where the non-phosphorylated form can passively diffuse into the cells.[21]

Pyridoxal 5'-phosphate and pyridoxal were then functionalized with thiosemicarbazide (**L1**, **L2**, **L4** and **L5**) or semicarbazide (**L3** and **L6**) (Figure 1). To screen the potential different biological behaviour, we decided to use the phosphorylated forms (**L1-L3**) to increase the water solubility of the compounds. The two methyl groups on the terminal nitrogen N^4 on **L2** and **L5** increased the hydrophobicity of the ligands and allowed us to explore the electron donating effect of these groups in the coordination behaviour of the metal. The synthesis of the semicarbazide derivatives **L3** and **L6** allowed us to study the influence of the oxygen as coordinating atom towards gallium(III). The chemical and antimicrobial properties of the compounds under study allowed us to explore their Structure-Activity Relationship (SAR). The compounds presented in this work were designed to be water soluble and we have characterized the ligands and their complexes in aqueous solution under physiological conditions. However, the importance of the speciation of metal complexes is known, and, in particular, studies of Ga(III) containing systems with similar biologically active ligands are found in the literature.[22] Here, we report our study on the protonation equilibria of the ligands and the speciation of the Ga(III)/L systems using UV/Vis spectrophotometric titrations.

Since WHO in 2017 made a list of priority pathogens for which new antibiotics are needed and at the high priority we found Gram negative bacteria which have developed resistance mechanism[23] we decided to test our compounds against a pool of resistant Gram negative bacteria, including two different strain of *Klebsiella pneumoniae* able to produce different type of β-lactamases (NDM-1 and ESβL), two different strains of *Escherichia coli* able to produce ESβL or biofilm, and a strain of *Pseudomonas aeruginosa* able to produce AmpC. For comparison, we included also a Gram positive strain clinically isolated, a *Vancomycin Resistant Enterococcus spp* another CIA resistance.

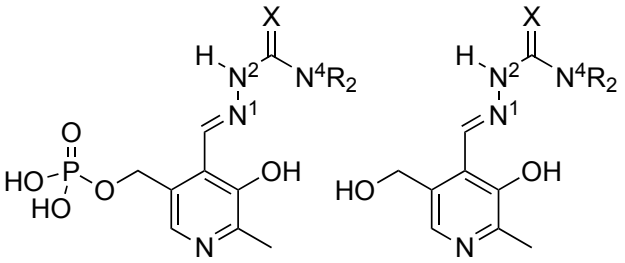

L1 X=S R=H
L2 X=S R=CH_3
L3 X=O R=H

L4 X=S R=H
L5 X=S R=CH_3
L6 X=O R=H

*Figure 1: Structure of the ligands with elucidation of the nitrogen numeration of the thiosemicarbazide (**L1-2**, **L4-5**) and semicarbazide (**L3**, **L6**) moiety.*

Materials and Methods

Materials

All common laboratory chemicals were purchased from commercial sources and used without further purification: thiosemicarbazide, 99% (Sigma Aldrich); semicarbazide hydrochloride, 99% (Alpha Aeser); 4,4-dimethyl-3-thiosemicarbazide, 98 % (TCI); pyridoxal-5-phosphate, 98.5 % (Merck); pyridoxal hydrochloride, 99 % (Alfa Aesar); $Ga(NO_3)_3 \cdot H_2O$, 99.9 % (Aldrich); potassium hydroxide, 85% (Sigma Aldrich), Sodium hydroxide pellets (Carlo Erba), Meropenem (Aldrich), Cefotaxime sodium salt (Aldrich). Triptic Soy Agar (TSA; Biolife Italiana, Milan, Italy) and Buffered Peptone Water (BPW; Biolife Italiana, Milan, Italy) were commercially available.

NMR were recorded on a Bruker Anova spectrometer at 400 MHz, with chemical shift reported in δ units (ppm). NMR spectra were referenced relative to residual NMR solvent peaks. Coupling constants (J) are reported in hertz (Hz). Solvent used in the spectra's acquisitions is DMSO-d_6, D_2O. NaOD was made starting from NaOH, with several cycles of dissolution/evaporation in D_2O. The FT-IR measurements were recorded on Perkin Elmer's Spectrum Two in the 4000-400 cm^{-1} range, equipped with the UATR accessory. Elemental analyses were performed using Flashsmart CHNS Elemental Analyzer (Thermofisher Scientific). ESI-MS were recorded on a spectrometer with Single Quadrupole Detector (Sesto San Giovanni, MI, Italy). HR-MS were recorded on a Thermo Scientific Orbitrap LTQ-XL (Rodano, MI, Italy). UV/Vis spectra were collected using a Thermofisher Scientific Evolution 260 Bio Spectrophotometer, using quartz cuvettes of 1 cm path length. Stock solution of the ligands (10 mM) and $Ga(NO_3)_3$ (10 mM) were freshly prepared in NaOH 0.1 M and HCl 0.1 M, respectively. Complexes was prepared in situ by mixing 1:1 the stock solutions of the ligands

and the metal. Stock solution of meropenem (2048 μgmL^{-1}) and cefataxime (2560 μgmL^{-1}) was dissolved in sterile water and stored at -18 °C. The 96-wells plates optical density was recorded at 620 nm by Multiskan FC Version 1.00.75 by Thermofisher Scientific. The plates containing selected bacteria strains were incubated in ICN200 Super ArgoLab at 37 °C.

Preparation of the ligands.

The thiosemicarbazones were synthetized from adapted known synthetic procedures.[24–26]

L1: Pyridoxal-5-phosphate (0.8 mmol, 201 mg) was completely dissolved in water (20 mL) under reflux. Thiosemicarbazide (0.8 mmol, 73.5 mg) was added. A bright yellow precipitate started to form. The reaction was stirred at room temperature for 8 more hours. The solid was filtered on filter paper, washed with cold ethanol, diethyl ether and dried under vacuum. Yellow powder. Yield: 80%. CHNS analysis $C_9H_{13}N_4O_5PS$. Calc: C 33.75, H 4.09, N 17.49, S 10.01. Found: C 33.90, H 4.22, N 17.15, S 9.65. ^{1}H NMR (400 MHz, D_2O, pH 13) δ 8.36 (s, 1H, NH-N=), 7.66(s, 1H, CH arom.), 4.86 (m, 2H, CH_2), 2.29 (s, 3H, CH_3). ^{13}C NMR (400 MHz, D_2O, pH 13) δ 176.30 (C=S), 160.38 (C-OH), 146.40 (C arom.), 143.37 (C=N), 133.59 (C arom.), 127.07(C arom.), 126.65(C arom.), 62.32(-CH_2-), 16.26(-CH_3). ^{31}P NMR (400 MHz, D_2O, pH 13) δ 3.76. ESI-MS (+, m/z, MeOH): calc. 343.0, found 343.2 [M+Na]$^+$. IR (ATR, cm^{-1}): 3354 cm^{-1}, 3283 cm^{-1}, 3142 cm^{-1} ν NH and ν OH; 1642 cm^{-1} ν C=N; 1585 cm^{-1} ν C=C, 1040 cm^{-1} ν N-C=S; 852 cm^{-1} ν C=S.

L2: Pyridoxal-5-phosphate (0.25 mmol, 624 mg) was dissolved in hot water (60 mL) with 1 mL of acetic acid. The mixture was kept under stirring and reflux until complete dissolution of the powder. Then 4,4'-dimethyl-3-thiosemicarbazide (301 mg, 0.25 mmol) was added. The formation of a yellow to orange precipitate started shortly after the addition of 4,4'-dimethyl-3-thiosemicarbazide. The reaction mixture was stirred at room temperature for 8 h. The solid was filtered on filter paper, washed with cold ethanol, diethyl ether and dried under vacuum. Yellow powder. Yield: 82 %. CHNS analysis $C_{11}H_{17}N_4O_5PS$. Calc: C 37.93, H 4.92, N 16.09, S 9.20. Found: C 37.66, H 4.90, N 15.82, S 9.36.^{1}H NMR (400 MHz, D_2O, pH 13) δ 8.51(s, 1H, NH-N=), 7.64 (s, 1H, CH arom.), 4.80 (m, 2H, CH_2), 3.16 (s, 6H, N-CH_3), 2.31(s, 3H, CH_3).^{13}C NMR (400 MHz, D_2O, pH 13) δ 181.46 (C=S), 168.36 (C-OH), 150.69 (C arom.), 146.16 (C=N), 134.47(C arom.), 131.99 (C arom.), 129.52 (C arom.), 61.77 (-CH_2-), 40.04 (N-CH_3), 18.20 (-CH_3).^{31}P NMR (400 MHz, D_2O, pH 13) δ 3.68. ESI-MS (+, m/z, MeOH): calc. 349.07, found 349.21 [M+H]$^+$; calc. 371.05, found 371.17 [M+Na]$^+$. IR (ATR, cm-1): 3167 cm^{-1}, 2987 cm^{-1} ν NH and ν OH; 1625 cm^{-1} ν C=N,1555 cm^{-1} ν C=C, 1098 cm^{-1} ν N-C=S, 841 cm^{-1} ν C=S.

L3: Pyridoxal-5-phosphate (1.43 mmol, 353 mg) were dissolved in hot water (13 mL) under reflux for 30 minutes. Semicarbazide hydrochloride (1.43 mmol, 160 mg) were dissolved in water (2 mL) and then slowly added to the reaction solution. A precipitate starts to form shortly after. The reaction was stirred at room temperature for 4 hours. The solid was filtered on filter

paper, washed with cold ethanol, diethyl ether and dried under vacuum. White precipitate. Yield: 88%. CHNS analysis $C_9H_{13}N_4O_6P$. Calc: C 35.54, H 4.31, N 18.42; Found: C 35.28, H 4.44, N 18.39. ^{1}H NMR (400 MHz, D_2O, pH 13) δ 8.20 (s, 1H, NH-N=), 7.69 (s, 1H, CH arom.), 4.79 (m, 2H, CH_2), 2.25 (s, 3H, CH_3). ^{13}C NMR (400 MHz, D_2O, pH 13) δ 196.01 (C=O), 160.22 (C-OH), 158.12 (C arom.), 151.70 (C arom.), 146.25 (C arom.), 141.16 (C=N), 61.95 (-CH_2-), 16.44 (-CH_3). ^{31}P NMR (400 MHz, D_2O, pH 13) δ 3.32.ESI-MS (+, m/z, MeOH): calc. 305.0, found 305.2 $[M+H]^+$. IR (ATR, cm^{-1}): 3376 cm^{-1}, 3160 cm^{-1} ν NH and ν OH; 1742 cm^{-1} ν CO; 1560 cm^{-1} ν C=C.

L4: Pyridoxal hydrochloride (0.9 mmol, 200 mg) and KOH (0.9 mmol, 59 mg) were dissolved in 20 mL of water at room temperature. Thiosemicarbazide (0.9 mmol, 82 mg) was then added. A precipitate starts to form shortly after. The reaction was stirred at room temperature for 4 hours and then filtered on paper filter. The solid was filtered on filter paper, washed with cold ethanol, diethyl ether and dried under vacuum. Yellow powder. Yield: 40%. CHNS analysis for $C_9H_{12}N_4O_2S$: C 44.99, H 5.03, N 23.32, S 13.34. Found: C 44.79, H 5.05, N 23.16, S 13.02.^{1}H NMR (400 MHz, DMSO-d_6): δ 11.61 ppm (s broad, 1H, NH=N), 9.67 ppm (s broad, 1H, phenolic OH), 8.58 ppm (s, 1H, CH=N), 8.33 ppm (s broad, 1H, NH_2), 8.10 ppm (s broad, 1H, NH_2), 8.0 ppm (s, 1H, CH arom.), 5.26 ppm (s, 1H, aliphatic OH), 4.59 ppm (s, 2H, CH_2), 2.41 ppm (s, 3H, CH_3).^{13}C NMR (400 MHz, DMSO-d_6): δ 149.56, 147.46, 142.50, 139.44, 133.35, 122.09, 59.40, 31.17, 19.60. ESI-MS (+, m/z, MeOH): calc. 263.3, found 263.1 $[M+Na]^+$. IR (ATR, cm^{-1}): 3440 cm^{-1}, 3374 cm^{-1}, 3260 cm^{-1}, 3160 cm^{-1}, 3090 cm^{-1} ν NH and ν OH, 1620 cm^{-1} ν C=N, 1528 cm^{-1} ν C=C, 1030 cm^{-1} ν N-C=S, 820 cm^{-1} ν C=S.

L5: Pyridoxal hydrochloride (3.3 mmol, 682 mg) and KOH (3.3 mmol, 157 mmol) were dissolved in 10 mL of hot MeOH. 4,4'-3-thiosemicarbazide (3.3 mmol, 398 mg) was then added. A precipitate starts to form shortly after. The reaction was stirred at room temperature for 8 hours. The solid was filtered on filter paper, washed with cold ethanol, diethyl ether and dried under vacuum. Yellow powder. Yield: 86 %. CHNS analysis for $C_{11}H_{16}N_4O_2S$: C 49.24, H 6.01, N 20.88, S 11.95. Found: C 49.11, H 6.16, N 20.83, S 12.16; ^{1}H NMR (400 MHz, DMSO-d_6): 12.38 ppm (s, 1 H, NH), 11.67 ppm (s, 1H, phenolic OH), 8.90 ppm (s, 1 H, CH=N), 7.94 ppm (s, 1H, CH arom.), 5.38 ppm (s, 1H, aliphatic OH), 4.60 ppm (s, 2H, CH_2), 2.42 ppm (s, 3H, CH_3), methyl peaks rely under water peak. ^{13}C NMR (400 MHz, DMSO-d_6): δ 181.64, 164.24, 150.36, 145.52, 132.46, 128.90, 127.53, 61.59, 38.84, 20.72. ESI-MS (+, m/z, MeOH): calc. 269.1, found 269.2 $[M+H]^+$; calc. 291.1, found 291.2 $[M+Na]^+$. IR (ATR, cm^{-1}): 3451 cm^{-1}, 3232 cm^{-1} ν NH and ν OH, 1678 cm^{-1} ν C=N, 1514 cm^{-1} ν C=C, 1046 cm^{-1} ν N-C=S, 806 cm^{-1} ν C=S.

L6: Pyridoxal hydrochloride (0.96 mmol, 196 mg) and KOH (0.96 mmol, 46 mg) were dissolved in 5 mL of water at room temperature. Semicarbazide hydrochloride (0.96 mmol,106 mg) were dissolved apart in water (2 mL) and then slowly added to the pyridoxal solution A precipitate starts to form shortly after. The reaction was stirred at room temperature for 4 hours. The solid

was filtered on filter paper, washed with cold ethanol, diethyl ether and dried under vacuum. White powder. Yield: 95%. CHNS analysis for $C_9H_{12}N_4O_p$: C 48.21, H 5.39, N 24.99; Found: C 48.31, H 5.46, N 25.14.^{1}H NMR (400 MHz, DMSO-d_6): 11.08 (s, 1H, NH), 8.40 (s, 1H, CH=N), 8.09 (s, 1H, CH arom.), 6.62 (s, 2H, NH_2), 5.62 (s broad, 1H, OH aliphatic), 4.69 (s, 2H, CH_2), 2.53 (s, 3H, CH_3). ^{13}C NMR (400 MHz, DMSO-d_6): δ 155.28 (C=O), 151.48 (C-OH), 144.15 (C arom.),137.36 (C=N), 135.28 (C arom.), 132.98 (C arom.), 127.05 (C arom.), 59.98 (-CH_2-), 16.58 (-CH_3); ESI-MS (+, m/z, MeOH): calc. 247.1, found 247.2 $[M+Na]^+$. IR (ATR, cm^{-1}): 3461 cm^{-1}, 3350 cm^{-1}, 3278 cm^{-1} , 3134 cm^{-1} ν NH and ν OH, 1699 cm^{-1} ν C=O, 1579 cm^{-1} ν C=C.

Preparation of the complexes

Stock solution of 3 mM Ga^{3+} complexes were freshly prepared in situ by mixing equimolar solution of $Ga(NO_3)_3$ dissolved in HCl 0.1M and the ligands dissolved in NaOH 0.1M. The pH of the resulting stock solution was neutral. Ga(III) complex solution were immediately used for antibacterial and cytotoxicity screening. The stock solutions were diluted 1: 200 with a mixture H_2O/MeOH 1:1 for HR-MS. Full HR-MS spectra are reported in Figure S1-S6.

GaL1: $[GaL1/C_9H11O_5N_4GaPS]^+$ calculated: 386.94436; found: 386.94381.

GaL2: $[GaL2/C_{11}H_{15}O_5N_4GaPS]^+$ calculated: 414.97566; found: 414.97511.

GaL3: $[GaL3/C_9H_{11}GaN_4O_6P]^+$ calculated: 370.96720; found: 370.96692: [GaL3-HCOOH/$C_{10}H_{13}GaN_4O_8P]^+$ calculated: 416.97268; found: 416.97213; [GaL3-HCOOH-HCOONa-$C_{11}H_{14}GaN_4NaO_{10}P]^+$ calculated: 484.96011; found: 484.95966; found: 416.97213; [GaL3-2HCOONa/$C_{11}H_{13}GaN_4Na_2O_{10}P]^+$ calculated: 506.94205; found: 506.94154. GaL3 has a high affinity for formic acid, and it ionizes with the track of the solvent in the source of ESI.

GaL4: [GaL4-H_2O / $C_9H_{12}GaN_4O_3S]^+$ calculated: 324.98859; found: 324.98804; [GaL4-CH_3OH/$C_{10}H_{14}GaN_4O_3S]^+$ calculated: 339.00424; found: 339.00369; [GaL4-Cl / $C_9H_{11}ClGaN_4O_2S]^+$ calculated: 342.95471; found: 342.95461; [GaL4-HCOOH / $C_{10}H_{12}GaN_4O_4S]^+$ calculated: 352.98351; found: 352.98324. GaL4 has a high affinity for formic acid, and it ionizes with the track of the solvent in the source of ESI.

GaL5: [GaL5-H_2O / $C_{11}H_{16}GaN_4O_3S]^+$ calculated: 353.01989; found: 353.01934; [GaL5-CH_3OH / $C_{12}H_{18}GaN_4O_3S]^+$ calculated: 367.03554; found: 367.03595; [GaL5-Cl / $C_{11}H_{15}ClGaN_4O_2S]^+$ calculated: 370.98601; found: 370.98659; [GaL5-HCOOH / $C_{12}H_{16}GaN_4O_4S]^+$ calculated: 381.01481; found: 381.01426. GaL5 has a high affinity for formic acid, and it ionizes with the track of the solvent in the source of ESI.

GaL6: [GaL6-H_2O / $C_9H_{12}GaN_4O_4]^+$ calculated: 309.01144; found: 309.01124; [GaL6-CH_3OH / $C_{10}H_{14}GaN_4O_4]^+$ calculated: 323.02709; found: 323.02679; [GaL6-Cl / $C_9H_{11}ClGaN_4O_3]$+ calculated: 326.97755; found: 326.97732.

. Microdilution MIC and MBC assay.

Klebsiella pneumoniae NDM-1 (NTCT14331); *Klebsiella pneumoniae* ESβL (NCTC13368), *Pseudomonas aeruginosa* clinical isolate (NCTC13713) were purchased from Star Ecotronics s.r.l. *Escherichia coli* ESβL, *Escherichia coli* biofilm, *Enterococcus spp*. *VRE* were isolated in the laboratory of Food Inspection of Parma University. The isolates were tested for their AMR profiles both phenotypically, through Kirby Bauer test, and genotypically by end-point PCR and Real time PCR technique. PCR allows the detection of the most common resistance genes in ESβL, AmpC, CRE and VRE bacteria.[27–30]

MIC (Minimum Inhibitory Concentration) and MBC (Minimum Bactericidal Concentration) values were determined by standard broth micro-dilution method following ISO 20776-1 (2019). Briefly, frozen stock bacteria were put into 5 mL of Buffered Peptone Water (BPW) and incubated for 2 h at 37 °C or until 0.5 McFarland. The bacterial density was adjusted to reach a final concentration of 5×10^5 $CFUmL^{-1}$. Tested antimicrobials were added in triplicate into 96-microwells plates, performing 2-fold serial dilution, followed by the addition of water (for antibacterial screening) or antibiotic (for combination therapy screening) and the prepared bacterial inocula. The plates were incubated at 37 °C for 18-24h. The MIC values were determined by OD reading at 620 nm using a spectrophotometer plate reader. MIC is the lowest concentration of a drug/broth dilution of antimicrobials that results in inhibition of the growth of the tested bacteria.[31] The MBC values were determined by transferring 100 µL of broth microdilution to a Triptic Soy Agar plate, a solid nonselective medium, and incubated at 37 °C for 18-24h. The MBC values were chosen as the lowest concentration of a drug/broth dilution of antimicrobials that results in killing 99.9% of the tested bacteria[31]. The Fractional Inhibitory Concentration Index (FICI) values were determined as follows: $FICI=FIC_A+FIC_B=C_A/MIC_A+C_B/MIC_B$, where MIC_A and MIC_B are the MIC values of compounds A and B alone, and C_A and C_B are the effective concentration of A and B when administrated. A FICI index of 0.5 or less indicates synergistic effect; between 0.5 and 4 the effect is additive. FICI index greater than 4 denotes antagonism.[32,33] The compounds were tested starting from the 1 mM. Meropenem and cefotaxime concentration were chosen following EUCAST 2021 guidelines and breakpoints table (MERO resistance MIC>8 μgmL^{-1} and CTX resistance MIC>2 μgmL^{-1}).[34]

UV/Vis spectroscopy

UV/Vis spectra were collected in the 250-450 nm range at 25 °C using quartz cuvettes of 1 cm path length. Spectrophotometric titrations of the ligands (C_L = 50 µM,) or of the ligands in the presence of Ga(III) (C_L = 50 µM, Ga:L = 1:1) 1:1 stoichiometry over a pH range between 3 and 11 at an ionic strength of 0.1 M KCl in water at 25 °C. The samples were prepared by diluting to 2.0 mL a proper amount of a 10 mM solution of L in 0.1 M NaOH solution, followed by addition of a proper amount of a 10 mM of gallium(III) nitrate in 0.1 M HCl. The pH was

corrected to 11 by addition of 0.1 M NaOH. The samples were titrated with a standard HCl 0.1 M solution, registering the UV/Vis spectrum of the solution for each titrant addition. The spectrophotometric titration curves were treated to determine the protonation (ligand titration) and the complex stability constants (Ga(III)/ligand titration). Data treatment was performed using the program Hypspec2014.[35] Speciation diagrams were calculated using the Hyss2009 software.[36]

Cytotoxicity

Human dermal fibroblasts HuDe were purchased from the Istituto Zooproflattico Sperimentale della Lombardia e dell'Emila (IZSLE) (Brescia, Italy). Cells were grown in RPMI 1640 medium containing 10% heat inactivated foetal bovine serum, 100 UmL^{-1} penicillin and 100 μgmL^{-1} streptomycin at 37 °C with 5% CO_2. Experiments were conducted with cells in the log phase growth. Cells (100000 mL^{-1}) were seeded into 96-well plates 24h and then exposed to compounds at concentrations between 0.1 μM and 100 μM. After incubation at 37°C for 24h cells were stained with Trypan Blue and counted with hemacytometer. At least three independent experiments were performed for each sample. Cell viability was assessed by the MTT (3-(4,5-dimethylthiazol-2-yl)-2,5-diphenyltetrazolium bromide) test, samples were read by spectrophotometer (Varioskan LUX Multimode Microplate Reader, Thermo Fisher Scientific).

Results and Discussion

The ligands were synthetized according to adapted general procedures previously reported.[24–26]. Briefly, the reaction is a condensation reaction between the two aldehydes, pyridoxal 5'-phosphate and pyridoxal, and the various thiosemicarbazides or semicarbazide. The reaction was conducted in methanol or water, based on the solubility of the reactants, with acetic acid as a catalyst. The compounds were characterised by ^{1}H NMR spectroscopy, ^{13}C NMR spectroscopy, ESI-MS, IR spectroscopy and elemental analysis. The corresponding Ga(III) complexes **GaL1**–**GaL6** were prepared in situ and characterized by UV/Vis spectroscopy and HR-MS.

The biological activity of the metal complexes is expected to strongly depend on the prevalent species at the physiological pH of 7.4. The distribution of the species at different pH is related to their relative stability, which, in turn, is related also to the proton dissociation constants of the coordinating donor groups. To determine the speciation of the gallium(III)/ligand systems, a series of pH-metric UV/Vis titrations were performed on solutions of the ligands and of the ligands in the presence of 1 eq. of Ga(III) nitrate. Alkaline solutions of the ligands and of the Ga(III)/L systems (pH ca. 11) were added with increasing amounts of HCl 0.1 M down to pH ca. 3. The UV/Vis spectra were collected after each titrant addition. Representative spectra

for the titration of **L5** and Ga(III)/**L5** are reported in Figure 2a and 2c. Treatment of the spectra dataset for the titration of the ligands allowed to determine the proton dissociation constants (K_a), which are reported in Table 1 in the form of pK_a. In Table 1 the logarithm of the global formation constants of the Ga(III) complexes (log β) are also reported along with the calculated conditional formation constants of the 1:1 **GaL1**-**GaL6** adducts at pH 7.4 (log K_{app}). The calculated molar UV/Vis spectra of the individual species can be found in supporting information (Figure S9) where also the logβ of the ligands are reported (Table S1).

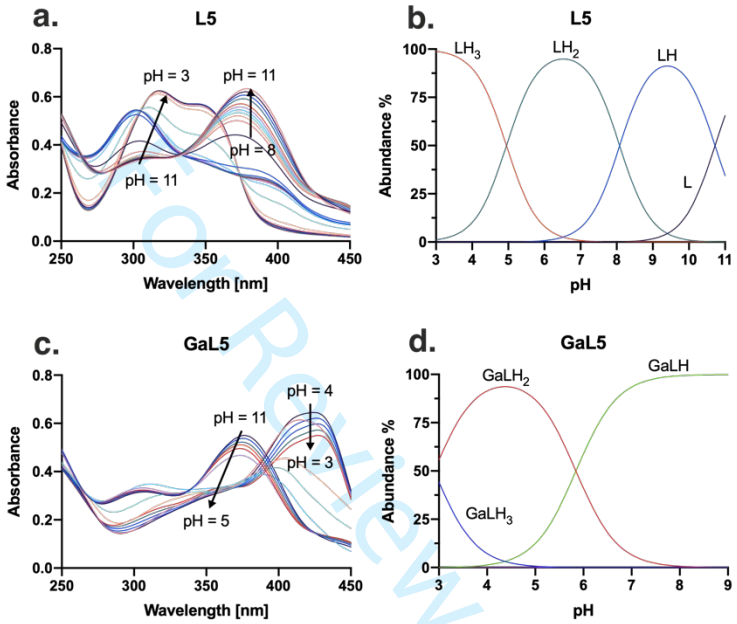

Figure 2. **a.** UV/Vis absorption spectra of **L5** at different pH (C_{L5} = 50μM). **b.** Representative species distribution diagram of **L5** (C_{L5} = 100μM). **c.** UV/Vis absorption spectra of the Ga^{3+}/**L5** system at different pH (C_{L5} = 50μM; Ga/**L5** = 1:1). **d.** Representative species distribution diagram of the Ga^{3+}/**L5** system (C_{L5} = 100μM; Ga/**L5** = 1:1). All experiments were performed in aqueous solution, T =298 K, I = 0.1 mol L^{-1} (KCl).

In their fully protonated forms, the pyridoxal phosphate derivatives **L1**-**L3** present four functional groups which can undergo proton dissociation in aqueous solution: the phosphate moiety (for two protons), the protonated pyridyl nitrogen, the phenolic OH and the N^2H of the (thio)semicarbazone moiety. Out of the corresponding five pK_a values for **L1** and **L2**, four of them could be determined by spectrophotometric data. The first pK_a of the phosphate group expectedly resulted too low to observe the proton dissociation equilibria in the experimental pH range. Evaluation of the data suggested that for all three **L1**-**L3** the pK_{a1} is lower than 2.5. Conversely, in the semicarbazone derivative **L3** the NH(C=O) group does not appreciably dissociate in water, and indeed consistently only three pK_a were determined in the experimental pH range of the titrations. On the other hand, the **L4**-**L6** ligands do not bear the phosphate group, and therefore only three pK_a values were expected and indeed found for **L4** and **L5**.

The determined pK_a values are in good agreement with those reported for similar compounds.[38,39] The deprotonation equilibria are represented, for **L5**, in Scheme 1, and a representative distribution diagram is reported in Figure 2b. As stated, in these ligands the first proton dissociation occurs at the phosphate group and could not be detected in the pH range investigated. The second proton dissociation (pK_{a2} = 4.1-4.9) likely occurs at the protonated pyridyl nitrogen, since pyridines functionalized with electron-withdrawing groups often present pK_a values lower than 5.[40] The third proton dissociation corresponds to the second dissociation at the phosphate group, which occurs close to the neutral pH (pK_a ca. 6), as expected. As for the last two dissociation steps, literature data suggest the phenol deprotonation occurs at lower pH than the thiosemicarbazide NH (pH 8 vs. 11.5). In the current series the ligands **L4**, **L5** and **L6** have the values of pK_{a4} and pK_{a5} fully consistent with the literature value. The pK_a values of **L1**, **L2** and **L3** for the dissociation of the phenolic OH site are spread over a quite large range of values, from 8.6 to 10.9, and their pK_{a5} values are much lower than 11.

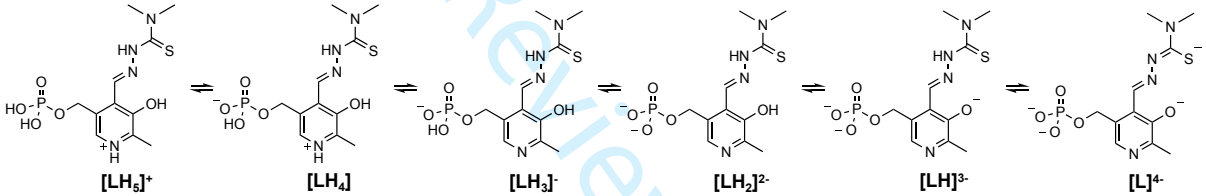

Scheme 1. Representative proton dissociation equilibria for **L5**.

The spectra dataset for the pH titration of the ligands in the presence of Ga(III) is different from that with the ligand alone at acidic and neutral pH. At alkaline pH (e.g. pH 11) the spectra are very similar, in agreement with the probable presence of uncomplexed ligand and Ga(III) in the form of hydroxo-species (see below). The spectra dataset were used to determine the stability constants of the gallium(III) complexes with the ligands using the pK_a values and the molar absorption spectra of the ligands in their different protonation forms as fixed parameters. With the purpose of accurate data treatment, the formation constants of the hydroxo-complexes of Ga(III) were also included in the calculations as fixed parameters.[37] The Ga(III)/ligand speciations are reported in Figure S8 while a representative spectrophotometric titrations and its corresponding species distribution diagram are shown in Figure 2c-2d.

The log β values of the Ga(III)/ligand adducts are reported in Table 1. The pH range reported in Table 1 refer to the pH range where the fitting of the spectral data could be obtained using the molar spectra of the different protonated forms of the ligand as fixed parameters, together with the related pK_a values. Within these pH ranges, five out of the six ligands form the $[GaLH_3]^{2+}$, $[GaLH_2]^{+}$ and [GaLH] species, the latter the prevalent species at pH 7.4 (Figure 3). For the **L1** ligand the [GaLH] specie was not detected, likely because a good fitting of the

spectral data could be obtained only below pH 6.3. Finally, with the **L2** which forms also a $[GaLH_4]^{3+}$ species.

In the absence of X-ray structural data, it is difficult to propose a coordination mode of the ligands to Ga(III). What data in Table 1 suggest, in particular the log K_{cond} values, is that the presence of the C=S or C=O does not play a major role in determining the stability of the adducts. While log K_{cond} are higher for **L3** in the **L1**-**L3** series (C=O in place of C=S), the opposite was observed for the **L4**-**L6** series. It is evident from the speciation data that almost all Ga(III) is present in the form of Ga(III) complexes and not of Ga(III) hydroxo-species (with the exception of **L1** for which no precise information at this pH can be obtained from species distribution). This evidence is indispensable for the further evaluation of their biological activity, in this case investigating their antimicrobial activities against multidrug-resistant bacteria and exploring their cytotoxicity.

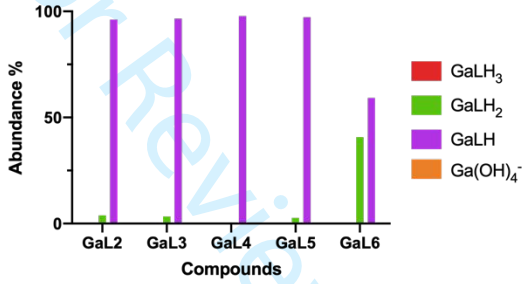

Figure 3. Calculated percentage of the relevant species at physiological pH of 7.4. Bars are not reported for the Ga/**L1** system since no precise information on the speciation at pH 7.4 is available.

The minimal inhibitory concentration (MIC) was evaluated in different Gram negative bacteria: *Klebsiella pneumoniae* (NTCT14331) that carries the bla_{NDM-1} metallo-carapenemase gene and was first isolated from human blood infection; *Klebsiella pneumoniae* (NCTC13368) that has the ability to produce Extended-Spectrum-β-Lactamases (ESβL) encoded by bla_{SHV-18} gene; *Pseudomonas aeruginosa* clinical isolate (NCTC13713) with an intrinsic upregulated AmpC β-lactamase activity. We tested the compounds also against a series of strains isolated in the laboratory of Food Inspection Unit of Parma University which include two Gram negative *Escherichia coli* ESβL (genes bla_{CTXM1}, bla_{CTXM2}, bla_{TEM} and bla_{SHV}) and a non-pathogenic *Escherichia coli* (phylogenetic group A), characterized by the ability to produce biofilm, and one Gram positive *Enterococcus spp* for which a resistant at vancomycin (VRE) was carried by VanA gene.

The lowest MIC values were recorded for **GaL2** and **GaL5**, which were active against all Gram negative bacteria tested (Table 2). The corresponding ligand **L2** and **L5** were also active, but with a higher MIC value. The compounds **GaL2** and **L2,** which presented the -OPO_3^{2-} moiety, were slightly less active in comparison to the compounds with the hydroxyl in the same position, indicating that compounds with higher charges may encounter more difficulties to get inside the cells. The active class of compounds **GaL2**, **L2**, **GaL5** and **L5** are thiosemicarbazones which present a doubly methylated N^4. The corresponding compounds with no substitution at N^4 were active only at high concentration, with no enhanced activity for gallium(III) compounds. Ligands **L2** and **L5** and their complexes **GaL2** and **GaL5** are more effective against the tested *E. coli* strains with respect *K. pneumoniae* strains. All the compounds were not active against the Gram positive bacteria tested, indicating that this group of compounds may be suitable for the development of antibacterial agents selective for Gram negative species. We also noted that all the semicarbazone derivatives **L3**, **GaL3**, **L6**, **GaL5** did not show any biological activity. Minimum Bactericidal Concentration (MBC) was also investigated but all the compounds showed only an inhibition of the growth with MBC values higher than the tested concentrations. Notably, the pure $Ga(NO_3)_3$ inorganic salt was not active, indicating once again that the properties observed are not the simple sum of those shown singularly by the metal and the ligand.

Klebsiella pneumoniae NDM-1 and Klebsiella pneumoniae ESβL were reference type culture (NCTC) and were chosen to test a combination therapy with our compounds and the antibiotics (meropenem and cefotaxime respectively). The MIC of the antibiotics were firstly investigated and secondly were evaluated with a sub inhibitory concentration of the synthetized compounds (MIC/4). The *Klebsiella pneumoniae NDM-1* produces a metallo β-lactamase able to hydrolyse the β-lactam of carbapenems and shows a meropenem MIC of 256 μgmL^{-1}. We noted that the pure ligands **L1-L6**, and the Ga(III) semicarbazone derivatives **GaL3**, **GaL6** did not show any activity. In the presence of the **GaL1**, **GaL2**, **GaL4** and **GaL5** the meropenem MIC lowered down to 64-32 μgmL^{-1}, with a Fractional Inhibitory Concentration Index (FICI) of 0.5 indicating a synergism between meropenem and the gallium complexes of the thiosemicarbazone ligands.[32,33] **GaL2** and **GaL5** have the best synergic effect because the effective concentration needed in the combination therapy is lower compared with the other compounds (Table 3). However, the synergism was not enough to restore carbapenem sensibility. Interestingly only Ga(III)-complexes showed synergism with the MBL-producing strain. Further studies may be needed to know the molecular target in the biological system and their possible inhibitory activity. *Klebsiella pneumoniae* ESβL which produces serine-β-lactamase (SHV-18) with cefotaxime MIC of 8 μgmL^{-1} did not show any relevant biological activity for the combination therapy of all the compounds.

The selectivity of our compounds against bacteria strains was evaluated studying the cytotoxicity effect against human epithelial HuDe cells that we used as model of eukaryotic cells. All the ligands and all the complexes exhibited no cytotoxicity after 24 hours from the treatment with IC_{50} > 100 μM. The morphology of the cell was also checked, and no significant difference was detected in comparison with the control lines. For this reason, the compounds have a high selectivity towards bacterial cells, showing no activity against the tested healthy human cells.

Conclusion

A series of ligands bearing a thiosemicarbazone or semicarbazone moiety, derived from pyridoxal and their respective 5'-phosphates have been synthesized and characterized. The speciation of the Ga(III)/ligand systems has been elucidated by UV/Vis spectrophotometric titrations, and the stability of the Ga(III)/L adducts calculated. For all the examined gallium(III)/ligand systems, at pH 7.4 Ga(III) is present only in the form of Ga(III) complexes. The compounds were then tested against different strains of *Klebsiella pneumoniae*, *Escherichia coli* and *Pseudomonas aeruginosa* which have developed different type of resistance mechanism including the production of β lactamase (NDM-1, ESβL or AmpC) or biofilm production. **GaL2** and **GaL5** showed an antibacterial activity against drug-resistant strains of Gram negative bacteria. **GaL2** and **GaL5** are gallium(III) complexes of thiosemicarbazone ligands which present a dimethylated N-terminal and present MIC values in the 62.5-15.63 μM range. The corresponding ligands **L2** and **L5** showed also antibacterial activity but with higher MIC values. We did not detect any growth inhibition in compounds derived from semicarbazide moieties **L3**, **GaL3**, **L6**, **GaL6**. The compounds were not active against the only Gram positive *Enterococcus spp.* tested. The combination therapy studies with NDM-1 producing *Klebsiella pneumoniae* showed synergism between meropenem and **GaL1**, **GaL2**, **GaL4** and **GaL5**. Since this group of compounds did not show any cytotoxicity against eukaryotic cells, they may be suitable for the developing of selective antibacterial agents for Gram negative bacteria.

Supplementary Data: Supporting information including experimental details are available.

Funding: This research was funded by the University of Parma (FIL).

Acknowledgments: This work has benefited from the equipment and framework of the COMP-HUB Initiative, funded by the 'Departments of Excellence' program of the Italian Ministry for Education, University and Research (MIUR, 2018–2022).

Conflicts of Interest: The authors declare no conflict of interest

References

1 A. Cassini, L. D. Högberg, D. Plachouras, A. Quattrocchi, A. Hoxha, G. S. Simonsen, M. Colomb-Cotinat, M. E. Kretzschmar, B. Devleesschauwer and M. Cecchini, *Lancet Infect. Dis.*, 2019, **19**, 56–66.

2 *Antimicrobial resistance surveillance in Europe 2022–2020 data*, World Health Organization, 2022.

3 Antimicrobial Resistance Collaborators, *Lancet*, 2022, 399, 629–655.

4 www.efsa.europa.eu/en/topics/topic/antimicrobial-resistance.

5 *Critically important antimicrobials for human medicine: categorization for the development of risk management strategies to contain antimicrobial resistance due to non-human antimicrobial use: report of the second WHO Expert Meeting, Copenhagen, 29-31 May*, World Health Organization, 2007.

6 M. Rega, I. Carmosino, P. Bonilauri, V. Frascolla, A. Vismarra and C. Bacci, *Microorganisms*, 2021, **9**, 214.

7 K. Hoelzer, N. Wong, J. Thomas, K. Talkington, E. Jungman and A. Coukell, *BMC Vet. Res.*, 2017, **13**, 1–38.

8 E. Barilli, A. Vismarra, V. Frascolla, M. Rega and C. Bacci, *J. Food Prot.*, 2020, **83**, 233–240.

9 A. Frei, J. Zuegg, A. G. Elliott, M. Baker, S. Braese, C. Brown, F. Chen, C. G. Dowson, G. Dujardin, N. Jung, A. P. King, A. M. Mansour, M. Massi, J. Moat, H. A. Mohamed, A. K. Renfrew, P. J. Rutledge, P. J. Sadler, M. H. Todd, C. E. Willans, J. J. Wilson, M. A. Cooper and M. A. T. Blaskovich, *Chem. Sci.*, 2020, **11**, 2627–2639.

10 J. L. Medina-Franco, E. López-López, E. Andrade, L. Ruiz-Azuara, A. Frei, D. Guan, J. Zuegg and M. A. T. Blaskovich, *Drug Discov. Today*, 2022, **xxx**, 1–11.

11 F. Minandri, C. Bonchi, E. Frangipani, F. Imperi and P. Visca, *Future Microbiol.*, 2014, **9**, 379–397.

12 J. A. Lessa, G. L. Parrilha and H. Beraldo, *Inorganica Chim. Acta*, 2012, **393**, 53–63.

13 A. Frei, *Antibiotics, 2020*.

14 Y. Wang, B. Han, Y. Xie, H. Wang, R. Wang, W. Xia, H. Li and H. Sun, *Chem. Sci.*, 2019, **10**, 6099–6106.

15 X.-M. Zhang, H. Guo, Z.-S. Li, F.-H. Song, W.-M. Wang, H.-Q. Dai, L.-X. Zhang and J.-G. Wang, *Eur. J. Med. Chem.*, 2015, **101**, 419–430.

16 G. Pelosi, S. Pinelli and F. Bisceglie, *Compd.* , 2022, 2.

17 M. Pioli, N. Orsoni, M. Scaccaglia, R. Alinovi, S. Pinelli, G. Pelosi and F. Bisceglie, *Molecules, 2021, 26*.

18 M. Scaccaglia, M. Rega, C. Bacci, D. Giovanardi, S. Pinelli, G. Pelosi and F. Bisceglie, *J. Inorg. Biochem.*, 2022.

19 F. Bisceglie, C. Bacci, A. Vismarra, E. Barilli, M. Pioli, N. Orsoni and G. Pelosi, *J. Inorg. Biochem, 2020.*

20 M. Pfanzelt, T. E. Maher, R. M. Absmeier, M. Schwarz and S. A. Sieber, *Angew. Chemie - Int. Ed.*, 2022, 1–11.

21 P. Acid, *Dietary Reference Intakes for Thiamin, Riboflavin, Niacin, Vitamin B6, Folate, Vitamin B12, Pantothenic Acid, Biotin, and Choline*, 1998.

22 S. Hakobyan, J.-F. Boily and M. Ramstedt, *J. Inorg. Biochem.*, 2014, **138**, 9–15.

23 WHO, Global priority list of antibiotic-resistant bacteria to guide research, discovery, and development of new antibiotics., www.who.int/news/item/27-02-2017-who-publishes-list-of-bacteria-for-which-new-antibiotics-are-urgently-needed.

24 M. Belicchi-Ferrari, F. Bisceglie, C. Casoli, S. Durot, I. Morgenstern-Badarau, G. Pelosi, E. Pilotti, S. Pinelli and P. Tarasconi, *J. Med. Chem.*, 2005, **48**, 1671–1675.

25 M. B. Ferrari, F. Bisceglie, E. Leporati, G. Pelosi and P. Tarasconi, *Bull. Chem. Soc. Jpn.*, 2002, **75**, 781–788.

26 M. B. Ferrari, F. Bisceglie, G. Pelosi, P. Tarasconi, R. Albertini, P. P. Dall'Aglio, S.

Pinelli, A. Bergamo and G. Sava, *J. Inorg. Biochem.*, 2004, **98**, 301–312.
27 D. Doyle, G. Peirano, C. Lascols, T. Lloyd, D. L. Church and J. D. D. Pitout, *J. Clin. Microbiol.*, 2012, **50**, 3877–3880.
28 N. Roschanski, J. Fischer, B. Guerra and U. Roesler, *PLoS One*, 2014, **9**, e100956.
29 F. J. Pérez-Pérez and N. D. Hanson, *J. Clin. Microbiol.*, 2002, **40**, 2153–2162.
30 F. E. Tatsing Foka and C. N. Ateba, *Biomed Res. Int.*
31 J. M. Andrews, *J. Antimicrob. Chemother.*, 2001, **48**, 5–16.
32 W. T. Langeveld, E. J. A. Veldhuizen and S. A. Burt, *Crit. Rev. Microbiol.*, 2013, **40**, 76–94.
33 R. Y. Huang, L. Pei, Q. Liu, S. Chen, H. Dou, G. Shu, Z. X. Yuan, J. Lin, G. Peng, W. Zhang and H. Fu, *Front. Pharmacol.*, 2019, **10**, 1–12.
34 www.eucast.org/clinical_breakpoints.
35 P. Gans, A. Sabatini and A. Vacca, *Talanta*, 1996, **43**, 1739–1753.
36 www.hyperquad.co.uk.
37 P. Persson, K. Zivkovic and S. Sjöberg, *Langmuir*, 2006, **22**, 2096–2104.
38 T. Jakusch, K. Kozma, É. A. Enyedy, N. V May, A. Roller, C. R. Kowol, B. K. Keppler and T. Kiss, *Inorganica Chim. Acta*, 2018, **472**, 243–253.
39 E. A. Enyedy, G. M. Bognár, N. V. Nagy, T. Jakusch, T. Kiss and D. Gambino, *Polyhedron*, 2014, **67**, 242–252.
40 R.M. Smith, A.E. Martell, R.J. Motekaitis, *NIST Critically Selected Stability Constants of Metal Complexes Database*, 2007.

*Table 1. Proton dissociation (pK_a) of the H^+ of the ligands **L1-L6** with overall stability (log β)[a] and conditional stability (log K_{cond})[b] constants of Ga(III) complexes formed with the ligands **L1-L6**. T = 25.0 °C, I = 0.10 M (KCl) in H_2O. The constant for hydrolytic cleavage for Ga^{3+} are $\log\beta_{GaH_{-1}}$ –3.93, $\log\beta_{GaH_{-2}}$ –7.73, $\log\beta_{GaH_{-3}}$ –12.38, $\log\beta_{GaH_{-4}}$ –15.96.*[37]

Species/pK_a	Functional gr.	L1	L2	L3	Functional gr.	L4	L5	L6
pK_a								
$[LH_5]^+$; pK_{a1}	$OP=O(OH)_2$	<2.5	<2.5	<2.5				
$[LH_4]$; pK_{a2}	Pyridyl NH^+	4.104(3)	4.82(2)	4.457(4)				
$[LH_3]^-$; pK_{a3}	$OP=O(O^-)(OH)$	6.098(7)	5.93(9)	5.97(2)	Pyridyl NH^+	4.066(2)	4.949(2)	4.551(2)
$[LH_2]^{2-}$; pK_{a4}	Phenolic OH	8.06(1)	7.39(7)	9.52(4)	Phenolic OH	8.048(4)	8.034(3)	8.603(8)
$[LH]^{3-}$; pK_{a5}	(C=S)NH	9.21(2)	8.71(1)	-	(C=S)NH	10.914(5)	10.720(8)	-
logβ								
$[GaLH_4]^{3+}$		45.1(3)	44.7(3)	–		–	–	–
$[GaLH_3]^{2+}$		41.1(3)	42.1(2)	44.61(3)		43.85(6)	43.64(9)	42.4(6)
$[GaLH_2]^+$		35.5(3)	36.9(2)	41.37(3)		39.72(6)	40.74(3)	38.1(6)
[GaLH]		-	30.9(3)	35.43(3)		34.67(5)	34.90(3)	30.8(6)
log K_{cond} (pH=7.4)		-	8.2(3)	12.27(3)		9.38(5)	9.78(3)	8.8(6)
pH range		3.2-6.3	3.0-7.4	2.8-9.3		3.5-8.5	3.3-8.9	3.3-7.7

[a] For the generic equilibrium pGa + qL + rH = $[Ga_pL_qH_r]$, $\beta = [Ga_pL_qH_r]/([Ga]^p\cdot[L]^q\cdot[H]^r)$; [b] K_{cond} = [Ga(III) bound to L]/([Ga(III) not bound to L]·[L not bound to Ga(III)])

Table 2: Antibacterial activity displayed as minimum inhibitory concentration (MIC; μM) against a panel of resistant bacteria strains

Bacteria	K. pneumoniae NDM-1	K. pneumoniae ESβL	E. coli ESβL	E. Coli biofilm	P. aeruginosa AmpC	Enterococcus spp VRE	HuDe[a]
L1	1000	500	>1000	500	500	>1000	>100
GaL1	>1000	>1000	>1000	250	>1000	>1000	>100
L2	500	250	500	31.25	125	>1000	>100
GaL2	62.5	62.5-31.25	15.63	15.63	31.25	>1000	>100
L3	>1000	>1000	>1000	>1000	>1000	>1000	>100
GaL3	>1000	>1000	>1000	>1000	>1000	>1000	>100
L4	1000	500	1000	500	500	>1000	>100
GaL4	>1000	500	500	500	500	>1000	>100
L5	250	125	250	31.25	125	>1000	>100
GaL5	31.25	31.25	15.63	15.63	62.5	>1000	>100
L6	>1000	>1000	>1000	>1000	>1000	>1000	>100
GaL6	>1000	>1000	>1000	>1000	>1000	>1000	>100
Meropenem	256*	-	-	-	-	-	-
Cefataxime	-	8*	16*	2*	32*	-	-
$Ga(NO_3)_3$	>1000	>1000	>1000	>1000	>1000	>1000	-

*[a] Cytotoxicity against HuDe cells as IC_{50} value. * μgmL^{-1}.*

Table 3: Minimum inhibitory concentration of the antibiotic* against resistant strains of *K. pneumoniae* in combination therapy with a sub inhibitory concentration of the compounds (MIC/4).

Bacteria	*K. pneumoniae NDM-1*		*K. pneumoniae ESβL*	
Compounds	*Effective concentration (MIC/4) [µM]*	*MIC meropenem [µgmL^{-1}]*	*Effective concentration (MIC/4) [µM]*	*MIC cefotaxime [µgmL^{-1}]*
L1	*250*	*>64*	*125*	*>4*
GaL1	*250*	*64*	*250*	*>4*
L2	*125*	*>64*	*62.5*	*>4*
GaL2	*15.63*	*64*	*15.63*	*>4*
L3	*250*	*>64*	*250*	*>4*
GaL3	*250*	*>64*	*250*	*>4*
L4	*250*	*>64*	*125*	*>4*
GaL4	*250*	*64*	*125*	*>4*
L5	*62.5*	*>64*	*31.25*	*>4*
GaL5	*7.81*	*64-32*	*7.81*	*>4*
L6	*250*	*>64*	*250*	*>4*
GaL6	*250*	*>64*	*250*	*>4*
$Ga(NO_3)_3$	*250*	*>64*	*250*	*>4*
*Antibiotic**	*-*	*256*	*-*	*8*

*Meropenem for *K. pneumoniae NDM-1*, cefotaxime for *K. pneumoniae ESβL*.

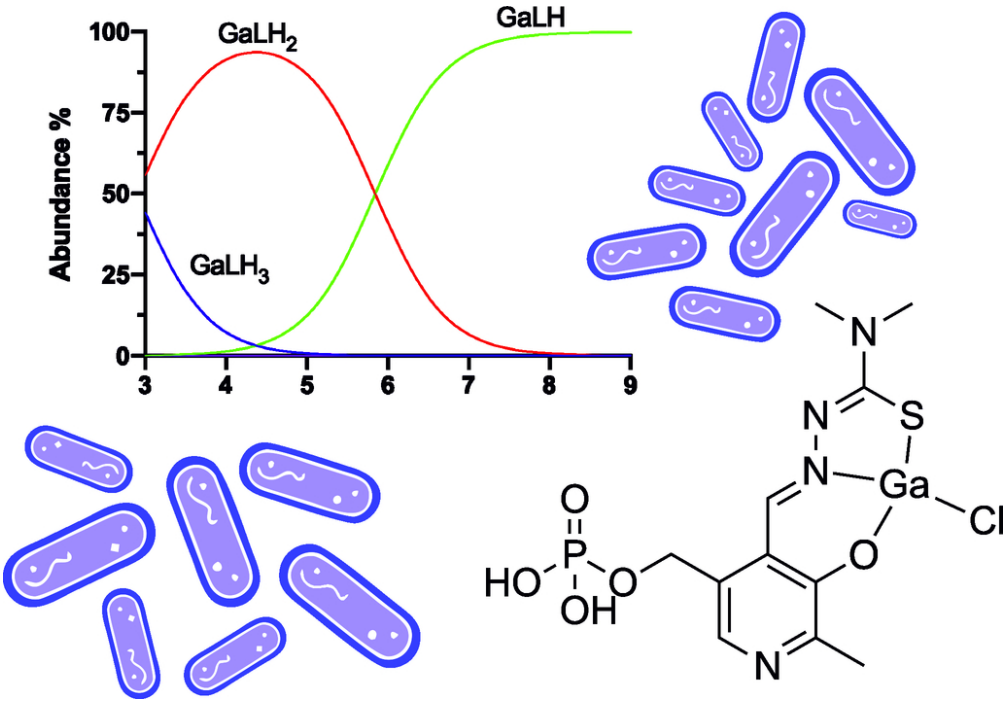

87x60mm (300 x 300 DPI)

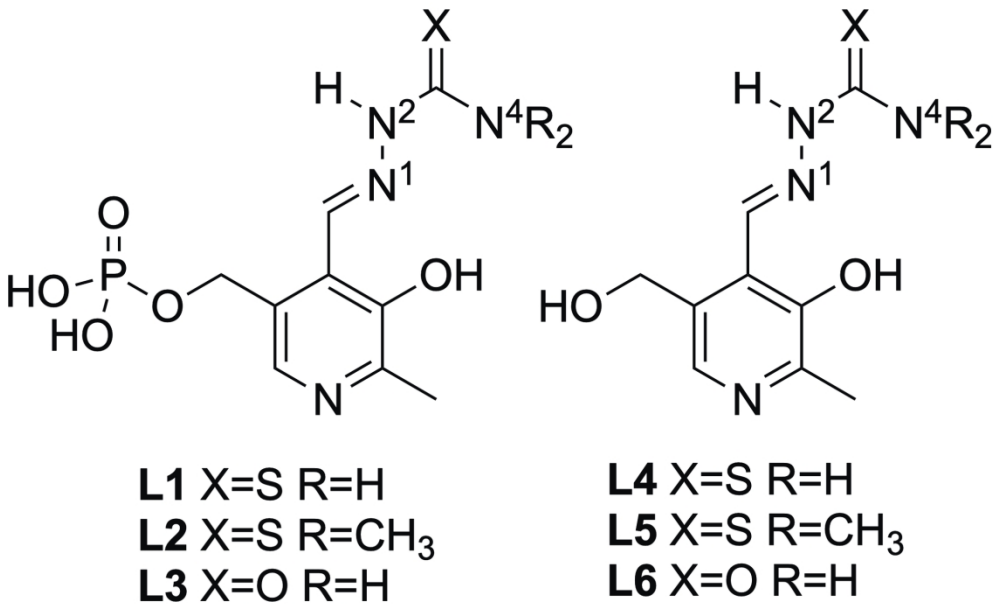

Structure of the ligands with elucidation of the nitrogen numeration of the thiosemicarbazide (L1-2, L4-5) and semicarbazide (L3, L6) moiety.

96x58mm (600 x 600 DPI)

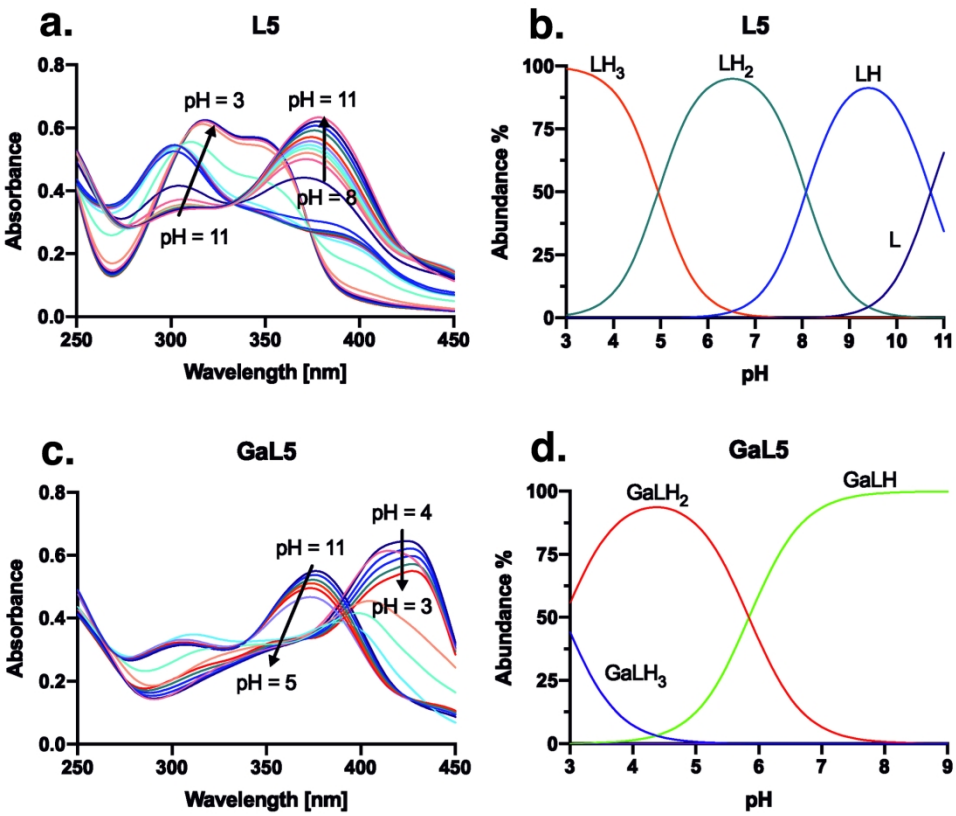

a. UV/Vis absorption spectra of L5 at different pH (C_{L5} = 50μM). b. Representative species distribution diagram of L5 (C_{L5} = 100μM). c. UV/Vis absorption spectra of the Ga3+/L5 system at different pH (C_{L5} = 50μM; Ga/L5 = 1:1). d. Representative species distribution diagram of the Ga3+/L5 system (C_{L5} = 100μM; Ga/L5 = 1:1). All experiments were performed in aqueous solution, T =298 K, I = 0.1 mol L^{-1} (KCl).

202x165mm (300 x 300 DPI)

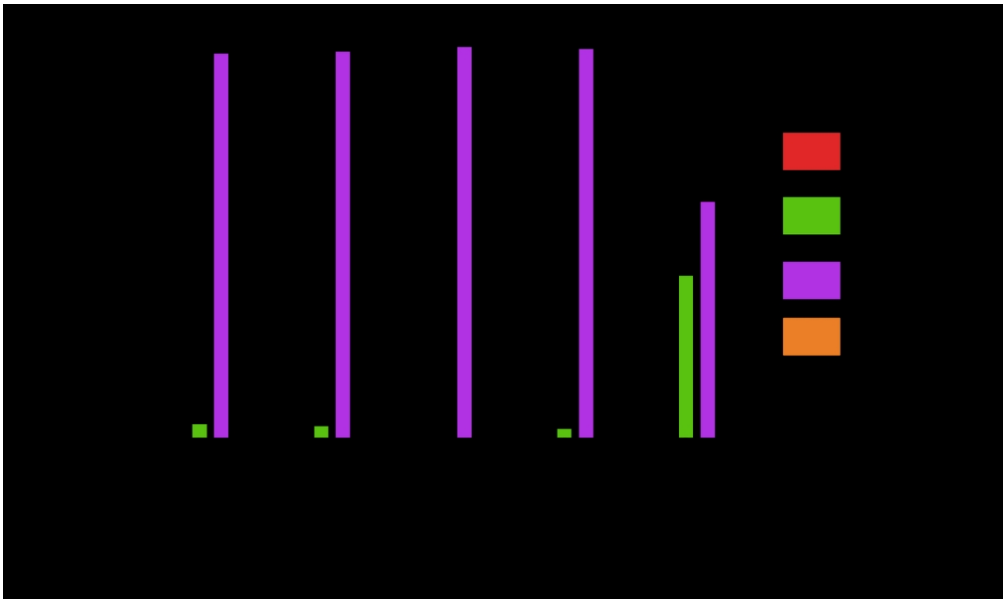

Calculated percentage of the relevant species at physiological pH of 7.4. Bars are not reported for the Ga/L1 system since no precise information on the speciation at pH 7.4 is available.

127x75mm (300 x 300 DPI)

Gallium(III)-Pyridoxal Thiosemicarbazone Derivatives as Nontoxic Agents against Gram Negative Bacteria

Mirco Scaccaglia[1], Martina Rega[2], Marianna Vescovi[1], Silvana Pinelli[3], Matteo Tegoni[1], Cristina Bacci[2], Giorgio Pelosi[1,4] and Franco Bisceglie[1,4]*

[1] Department of Chemistry, Life Sciences and Environmental Sustainability, University of Parma, 43124 Parma, Italy;

[2] Department of Veterinary Science, University of Parma, Strada del Taglio 10, 43126 Parma, Italy;

[3] Department of Medicine and Surgery, University of Parma, Via Gramsci 14, 43126 Parma, Italy;

[4] CERT, Center of Excellence for Toxicological Research, University of Parma, 43124 Parma, Italy

* corresponding author: franco.bisceglie@unipr.it

Supporting information

GaL1

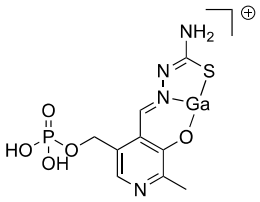

$C_9H_{11}GaN_4O_5PS$

GaL2

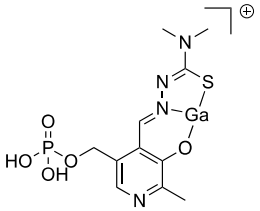

$C_{11}H_{15}GaN_4O_5PS$

GaL3

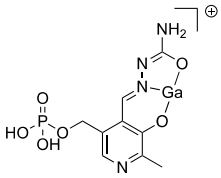

$C_9H_{11}GaN_4O_6P$

GaL3-HCOOH

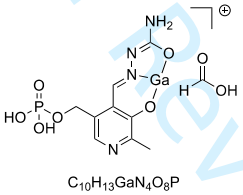

$C_{10}H_{13}GaN_4O_8P$

GaL3-HCOOH-HCOONa

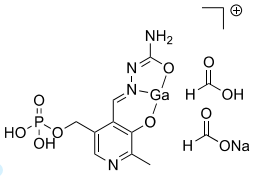

$C_{11}H_{14}GaN_4NaO_{10}P$

GaL3-2HCOONa

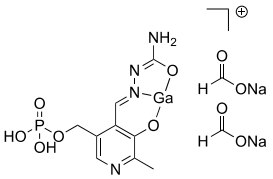

$C_{11}H_{13}GaN_4Na_2O_{10}P$

GaL4-H_2O

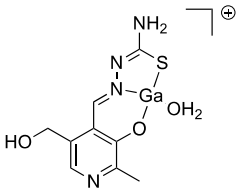

$C_9H_{12}GaN_4O_3S$

GaL4-CH_3OH

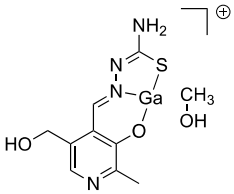

$C_{10}H_{14}GaN_4O_3S$

GaL4-Cl

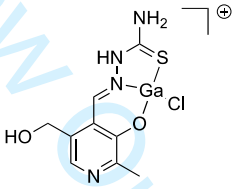

$C_9H_{11}ClGaN_4O_2S$

GaL4-HCOOH

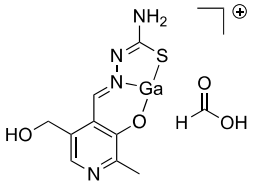

$C_{10}H_{12}GaN_4O_4S$

GaL5-H_2O

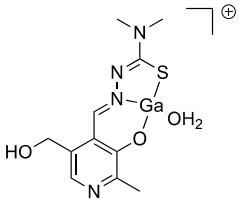

$C_{11}H_{16}GaN_4O_3S$

GaL5-CH_3OH

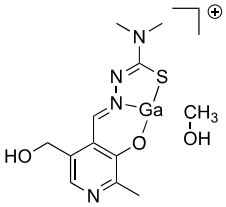

$C_{12}H_{18}GaN_4O_3S$

GaL5-Cl

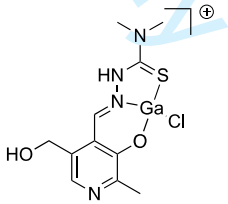

$C_{11}H_{15}ClGaN_4O_2S$

GaL5-HCOOH

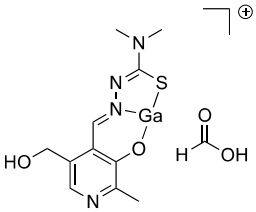

$C_{12}H_{16}GaN_4O_4S$

GaL6-H_2O

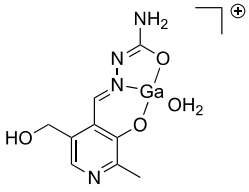

$C_9H_{12}GaN_4O_4$

GaL6-CH_3OH

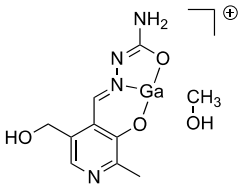

$C_{10}H_{14}GaN_4O_4$

GaL6-Cl

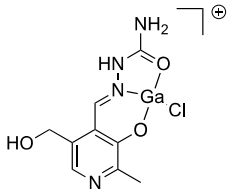

$C_9H_{11}ClGaN_4O_3$

Scheme S1: Scheme of the molecular structure of the relevant ions detected with full HR-MS.

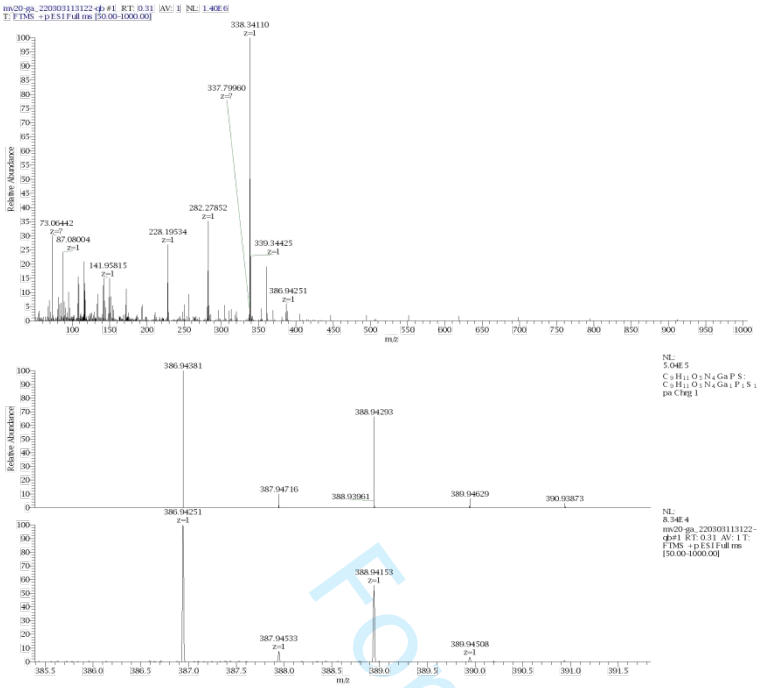

Figure S1. Full HR-MS of GaL1.

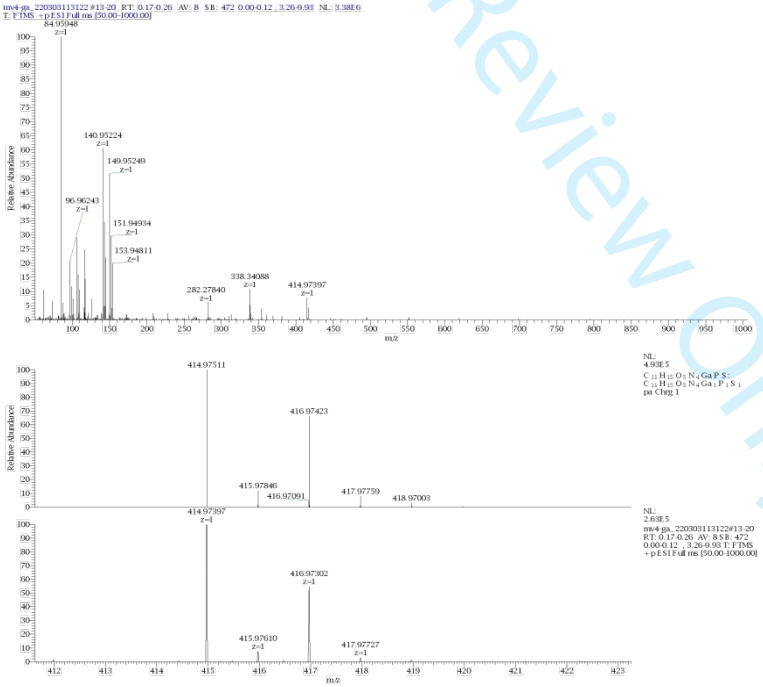

Figure S2. Full HR-MS of GaL2

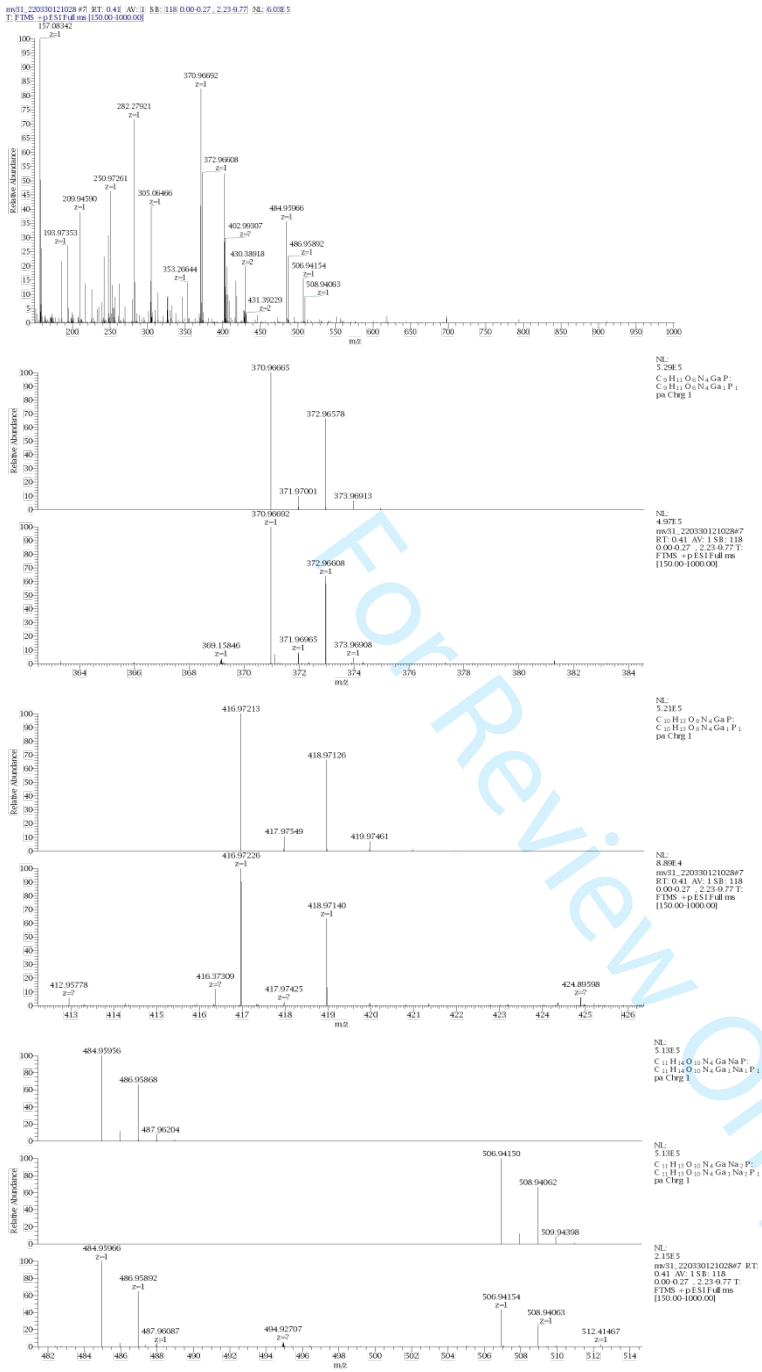

Figure S3. Full HR-MS of GaL3

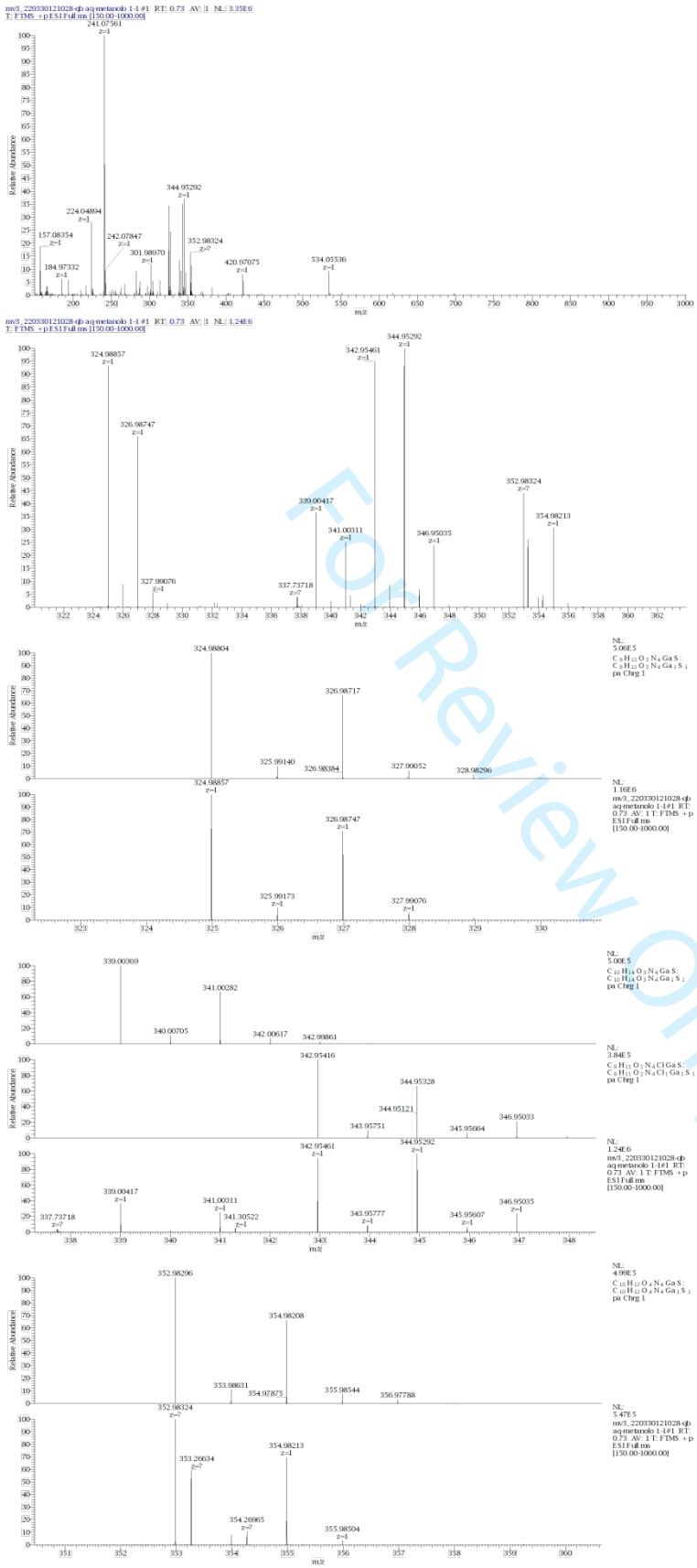

Figure S4. Full HR-MS of GaL4

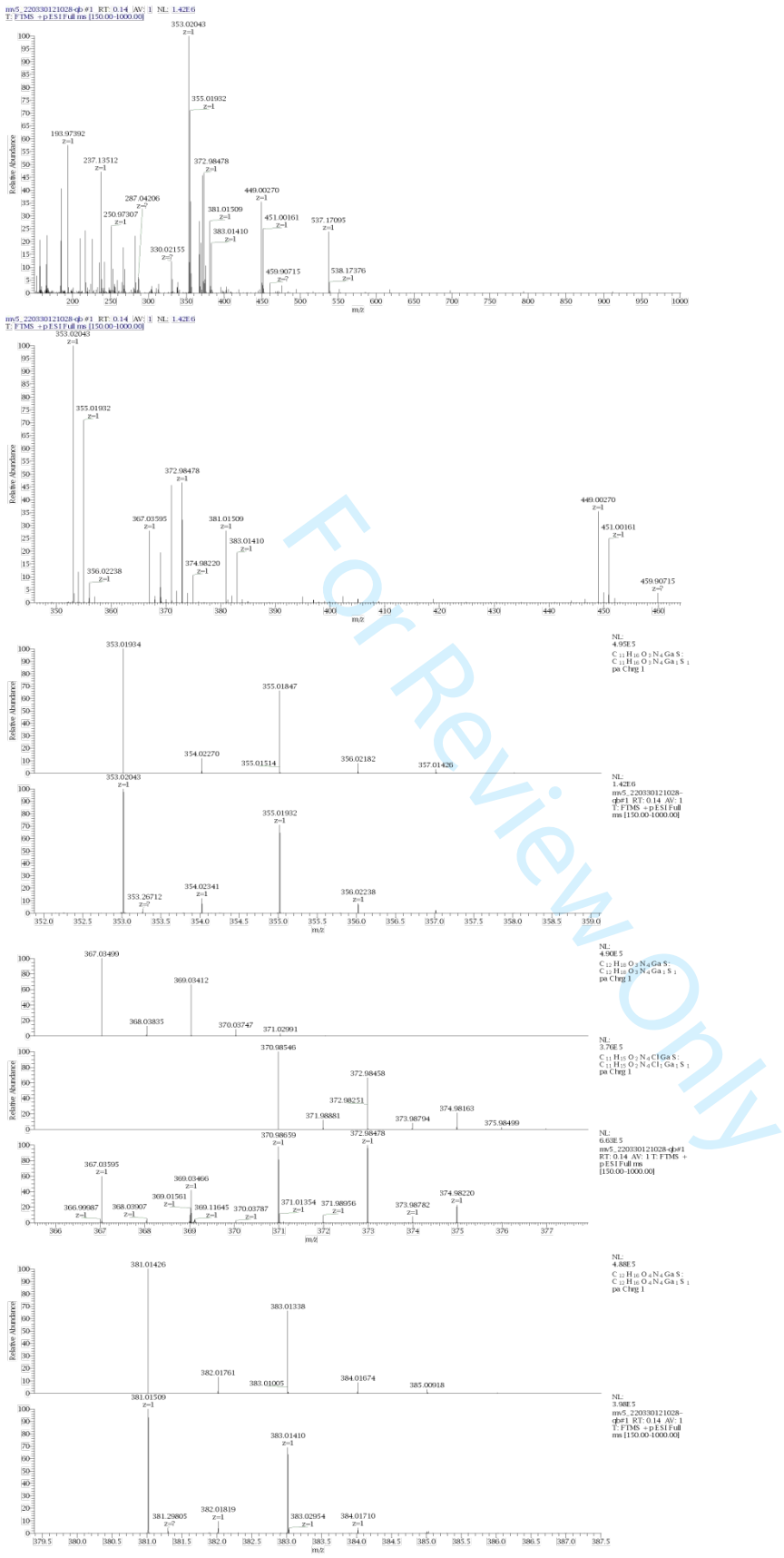

Figure S5. Full HR-MS of GaL5

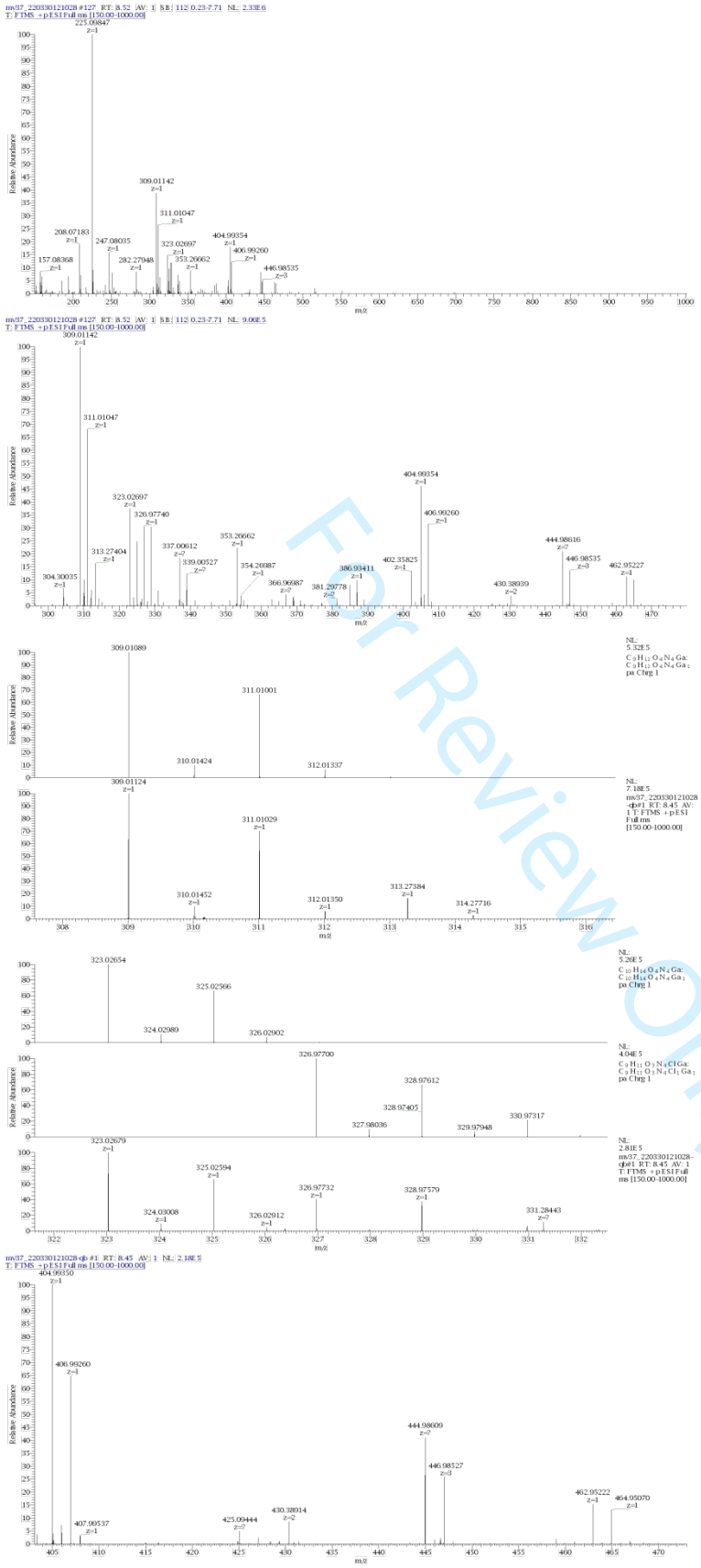

Figure S6. Full HR-MS of GaL6

Table S1. Overall stability (log β)[a] of the H^+ of the ligands **L1**-**L6**. T = 25.0 °C, I = 0.10 M (KCl) in H_2O.

Species	L1	L2	L3	L4	L5	L6
$[LH]^{3-}$	9.21(2)	8.71(1)	9.526(4)	10.914(5)	10.720(8)	8.603(8)
$[LH_2]^{2-}$	17.27(5)	16.11(6)	15.50(2)	18.963(6)	18.804(9)	13.154(9)
$[LH_3]^{-}$	23.37(3)	22.0(1)	19.96(2)	23.029(6)	23.752(9)	–
$[LH_4]$	27.47(3)	26.8(1)	–			

[a] For the generic equilibrium $L + rH = [LH_r]$, $\beta = [LH_r]/([L]\cdot[H]^r)$

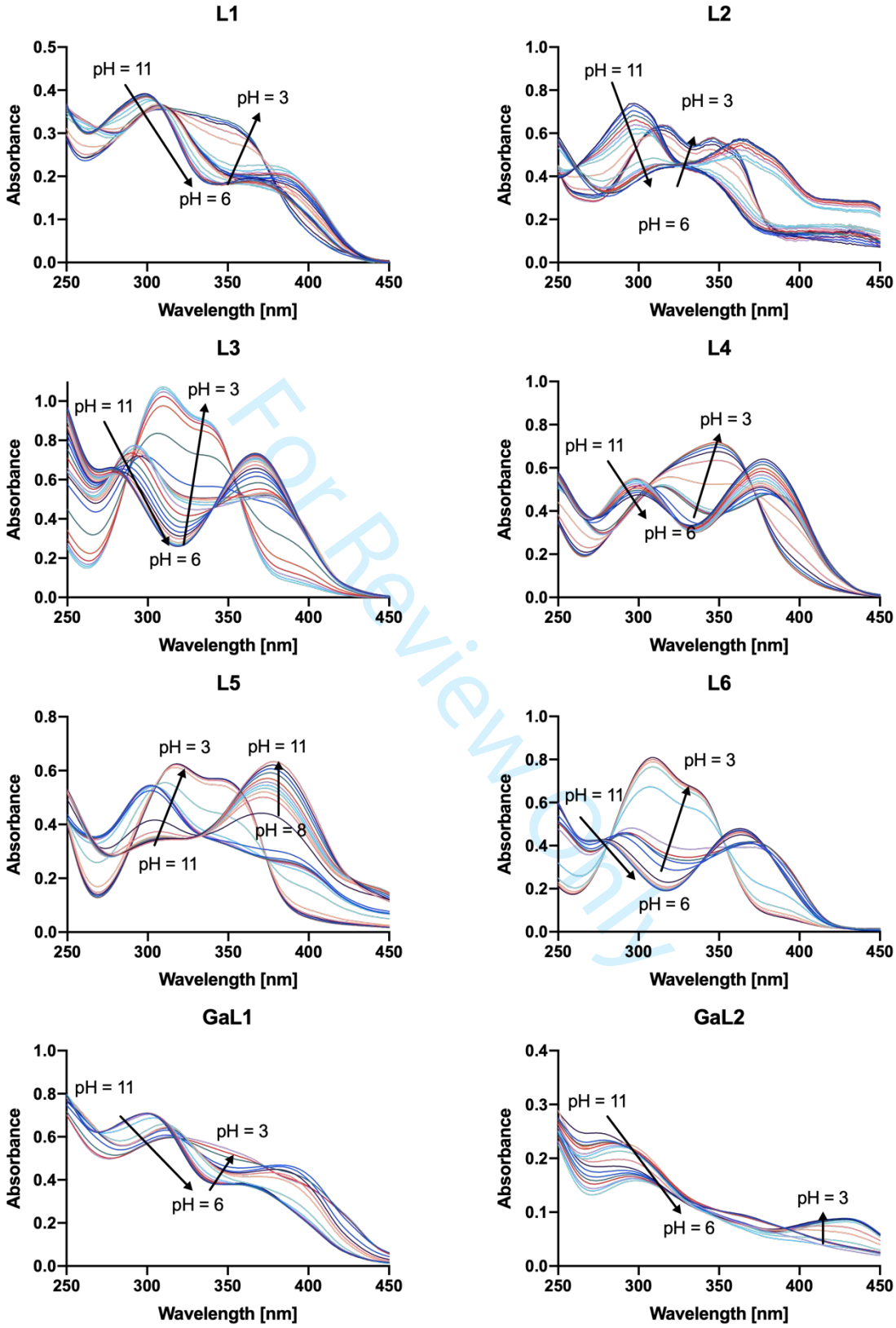

Figure S7. (continued on next page)

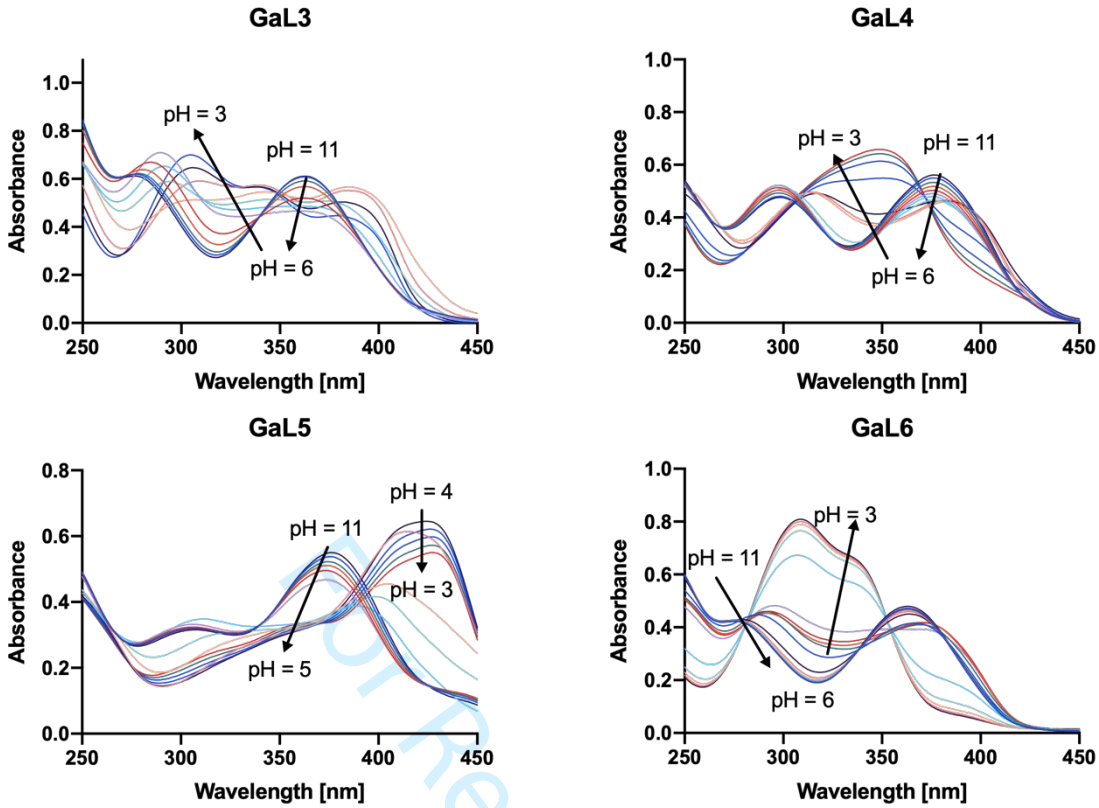

Figure S7. UV-Vis absorption spectra of ligans **L1**-**L6**(C_L = 50μM) and of the Ga^{3+}/**L1**-**L6** (C_L = 50μM; Ga/**L** = 1:1) system at different pH. All experiments were performed in aqueous solution, T =298 K, I = 0.1 mol L^{-1} (KCl).

Speciation diagram of the ligands.

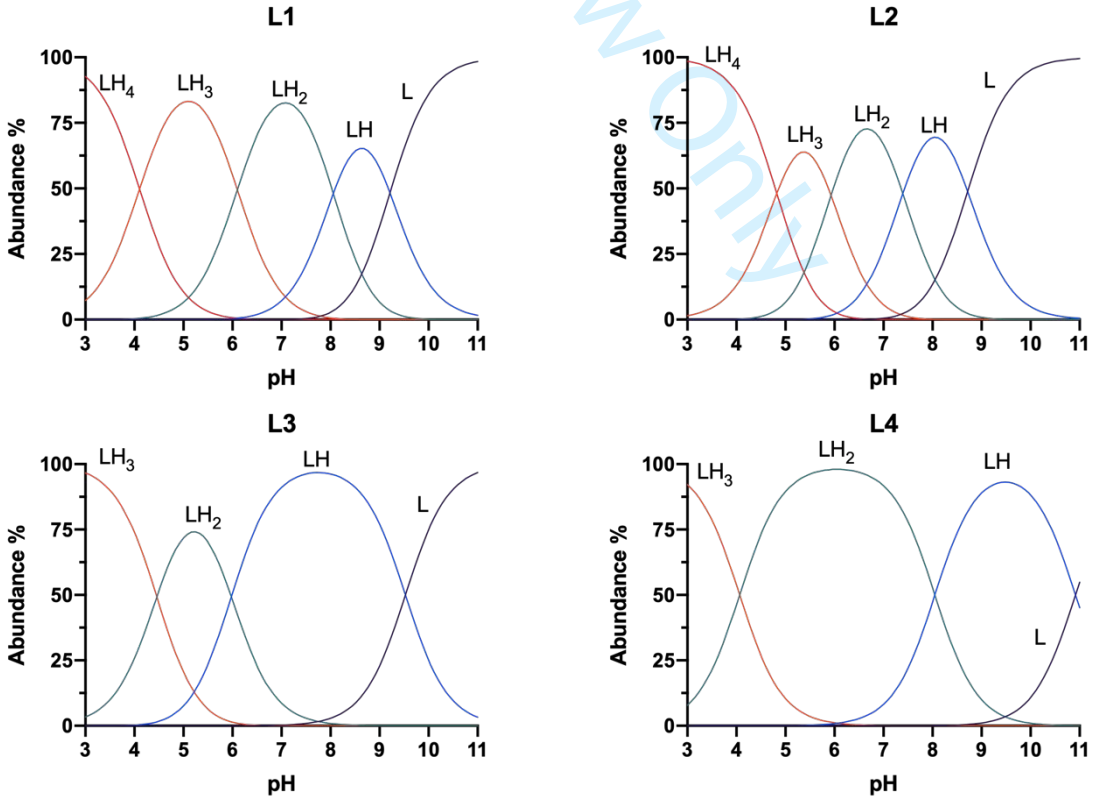

Figure S8. (continued on next page)

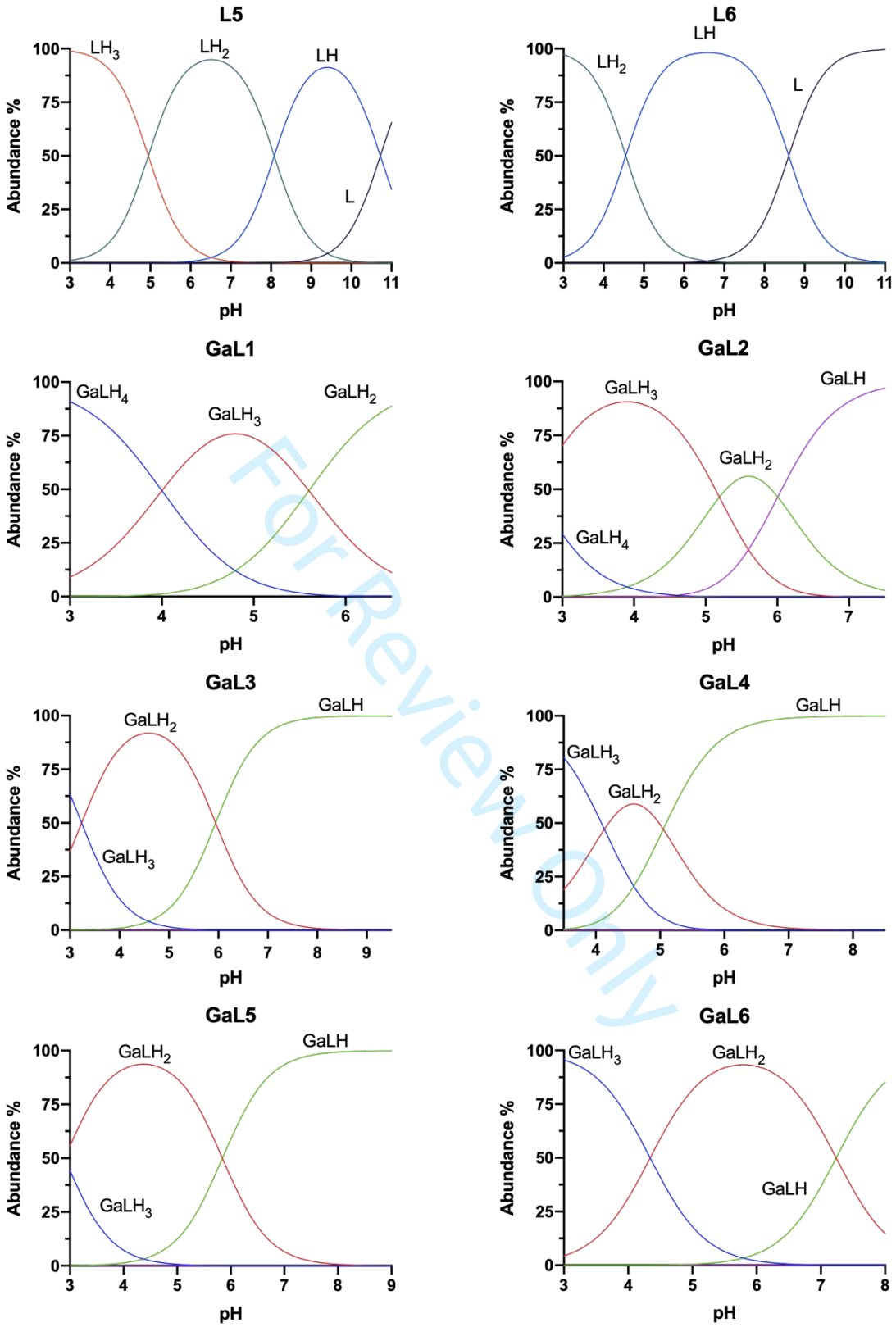

Figure S8. Representative species distribution diagram of **L1**-**L5** (C_L = 100 μM) and of the Ga^{3+}/**L1**-**L5** system (C_L = 100 μM; Ga/**L** = 1:1). All experiments were performed in aqueous solution, T =298 K, I = 0.1 mol L^{-1} (KCl).

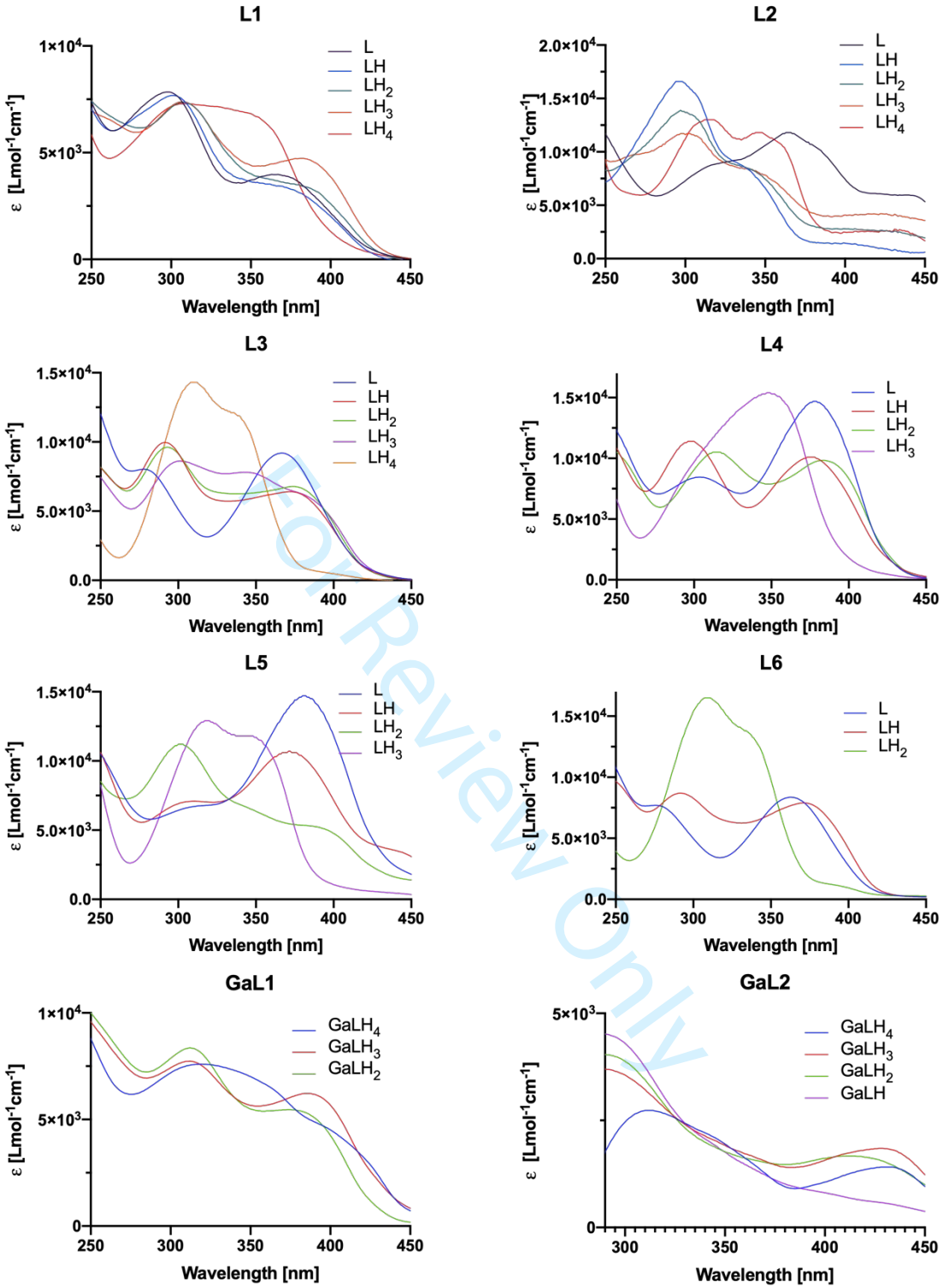

Figure S9. (continued on next page)

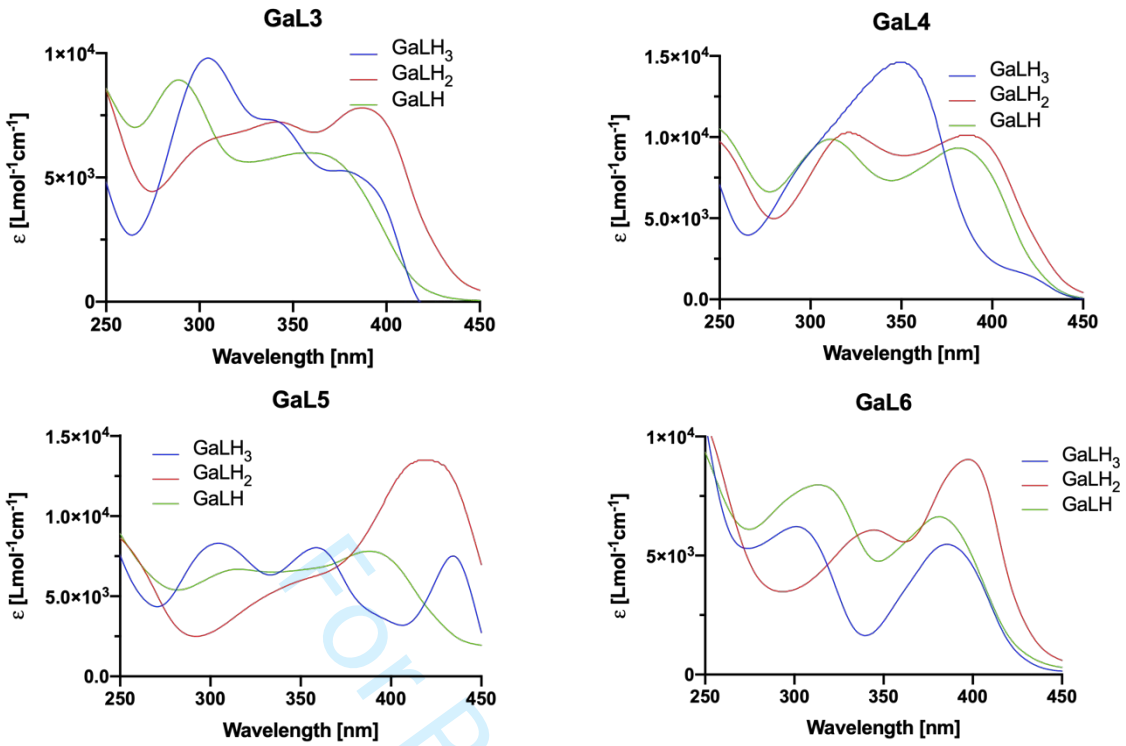

Figure S9. Calculated molar UV–Vis spectra of the different protonated species of **L1**-**L6** and **GaL1**-**GaL6**.